Serviceability Design of Continuous Prestressed Concrete Structures

Amin Ghali
Professor of Civil Engineering
The University of Calgary
Calgary, Alberta, Canada

Mamdouh M. Elbadry
Post-Doctoral Fellow
Department of Civil Engineering
The University of Calgary
Calgary, Alberta, Canada

Concrete structures reinforced with or without prestressing are designed to satisfy the requirements of safety against failure and serviceability. Safety against failure can be assessed by estimating the ultimate load that can be carried by the structure. This check is relatively simple and is beyond the scope of this paper. But to ensure the serviceability requirements, it is essential to predict the stresses and deformations of the structure under service load conditions.

Stresses and deformations vary continuously with time due to the effects of creep and shrinkage of concrete and relaxation of prestressed steel. These effects lead to a redistribution of stresses between various materials within a cross section and to a change in reactions, and hence, a change in the internal forces if the structure is statically indeterminate. The importance of these time-dependent effects is much more pronounced in structures built in stages than in those constructed in one operation. Examples of such structures are continuous bridges built span by span; segmental construction; and bridges built of precast prestressed concrete members connected and made continuous by cast-in-place concrete deck or joints and a subsequent prestressing.

Under increasing service loads, cracking occurs when the tensile strength of concrete is exceeded, resulting in further redistribution of stresses in individual sections, a considerable reduction in stiffness of different members and important changes in deformations. In statically indeterminate structures, the changes in member stiffnesses can result in changes in reactions and internal forces.

In current practice, the initial prestressing forces are treated as external forces applied on a plain concrete structure. The time-dependent change

in prestressing force, commonly referred to as the prestress loss, is estimated and its effect is treated in the same way as the initial prestressing force. The variation of the prestress loss from section to section is commonly ignored. Prestressed structures generally contain a considerable amount of nonprestressed steel. The presence of this steel, although frequently ignored, has a significant effect on the time-dependent redistribution of stresses between concrete and steel. Therefore, it is important to account for the time-dependent stress changes in both prestressed and nonprestressed steels.

Several methods and computer programs are available in the literature for the time-dependent analysis of segmental constructions and structures built in stages.[1-9] However, none of these methods and programs includes the effect of cracking under increasing service loads.

In this paper, a numerical procedure is presented and a computer program is described for the analysis of reinforced concrete plane frames with or without prestressing. The analysis gives the instantaneous and time-dependent changes in the displacements, in support reactions and in statically indeterminate internal forces. It also gives the corresponding changes in stress and strain at various sections of the structure.

The analysis accounts for the effects of creep and shrinkage of concrete and relaxation of prestressed steel, for the effects of sequence of construction and change of geometry and support conditions, for the effects of temperature variations and movement of supports, and for the effects of cracking. An estimate of the average crack width is also made. With segmental construction and other multi-stage casting and prestressing procedures, the analysis gives the history of stresses and deformations.

Cracking drastically reduces the stresses and internal forces induced by temperature variations or support movements and thus should not be ignored. This is discussed in a separate paper.[10]

In the analysis presented herein, the approximate estimate of the time-dependent prestress loss is avoided. Instead, the conditions of equilibrium of forces and compatibility of strains in the

Synopsis

An efficient numerical procedure is presented and reference is made to an available computer program for the analysis necessary in the design for serviceability of reinforced concrete plane frames with or without prestressing. Applications include continuous bridges and building frames.

The procedure accounts for the effects of creep and shrinkage of concrete and relaxation of prestressed steel. The effects of cracking, particularly on the deflections, the reactions and the internal forces in statically indeterminate structures, are also considered.

A frame member can be made up of concrete parts of different properties constructed in different stages or of concrete and structural steel. Material properties and ages can vary also from one member to another, as in the case of segmental construction.

Instantaneous and time-dependent changes in stress and strain in individual sections are calculated using one set of equations applicable to both cracked and noncracked states. The computer program is simple and can be routinely employed in checking the design of reinforced and prestressed concrete structures for serviceability requirements using a microcomputer. Two bridge examples are presented to demonstrate the applicability of the program.

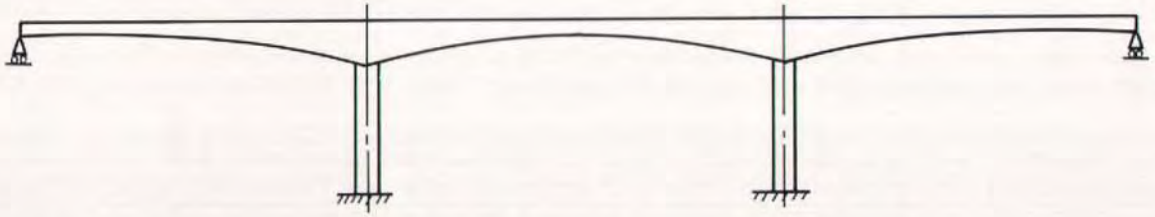

Fig. 1. Typical reinforced or prestressed concrete plane frame.

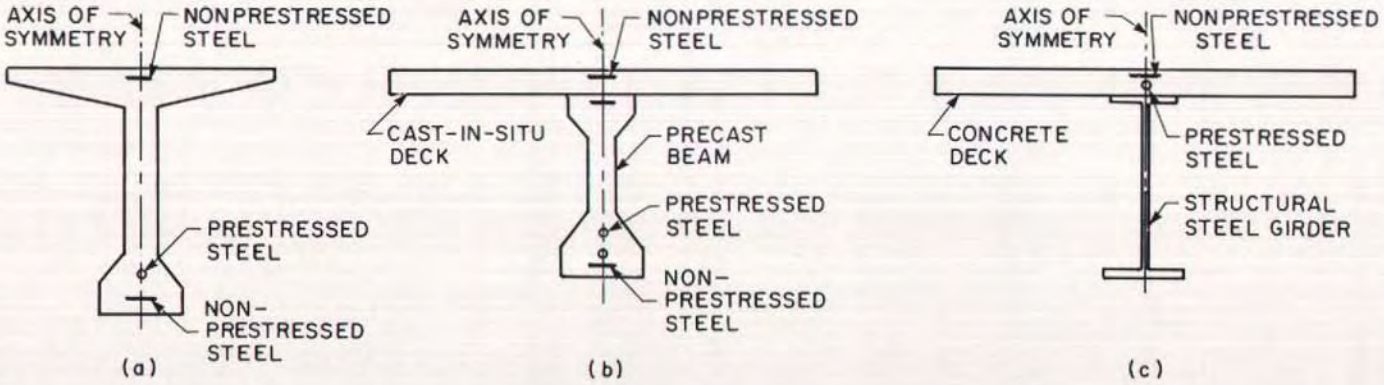

Fig. 2. Typical cross sections treated in the present analysis.

concrete and steel in any section are employed to determine the changes in strain and in forces in each of these components.

The input data for prestressing is simply the magnitude of the initial prestressing force and the locations of the tendons at various sections. When post-tensioning is employed, the loss in the jacking force due to friction and anchorage slip is taken into account. The so-called balancing forces exerted on concrete wherever a prestressing tendon changes direction are automatically included and need not be calculated by the analyst.

The assumptions adopted in the analysis concerning the structural discretization and the stress-strain relations are given in the following sections. Two numerical examples are presented to illustrate the applicability and the practicality of the proposed method.

STRUCTURAL AND TEMPORAL DISCRETIZATION

The analysis is based on the displacement method[11] in which a plane frame is idealized as an assemblage of straight beam elements connected at the joints (nodes). The axes of the beams lie in one plane and the external applied loads act in the same plane, at the nodes or on the axes of the members. The centroid of a transformed cross section of a member changes position with time due to varying concrete properties and due to cracking. For this reason, a reference axis is arbitrarily chosen for each element and is kept unchanged through all steps of the analysis. The nodes of the frame are located at the intersection of the reference axes of individual elements.

A member of the frame can be of constant or variable depth (Fig. 1). The member cross section can consist of several concrete parts of different types or of concrete and structural steel (Fig. 2). A concrete part can be divided into a set of rectangles or trapeziums for which the dimensions are specified. When a section has a structural steel part or a standard precast element, the area properties and height of this part are entered as data instead of its detailed dimensions. A cross section can also contain more than one layer of prestressed or nonprestressed steel reinforcements. A prestressed tendon can be pretensioned or post-tensioned and is represented by a series of straight line and parabolic segments. A prestressed or nonprestressed steel layer can extend over a portion or over the full length of the member.

The time is divided into intervals; the instant t_i at the start of interval i coincides with the addition of new members or new parts of a member, with the application of load or prestressing, or with the change in support conditions. For each time interval, the analysis gives the instantaneous and time-dependent changes in three nodal displacement components: two translations and a rotation (Fig. 3a), three forces at the two ends of individual members (Fig. 3b) and the reactions at the supports. The corresponding changes in stress and strain in individual cross sections are calculated using methods[12,13,14] which are reviewed here.

Deformations due to shear are ignored, while those due to bending and axial force are taken into account. External loads can be in the form of forces or couples applied at the nodes (Fig. 4a), concentrated loads or couples at any point on the axis of the member or a distributed load of any variation covering a part or the full length of the member (Fig. 4b).

INITIAL PRESTRESSING FORCE

In pretensioned members, the input must include the tension in the tendons

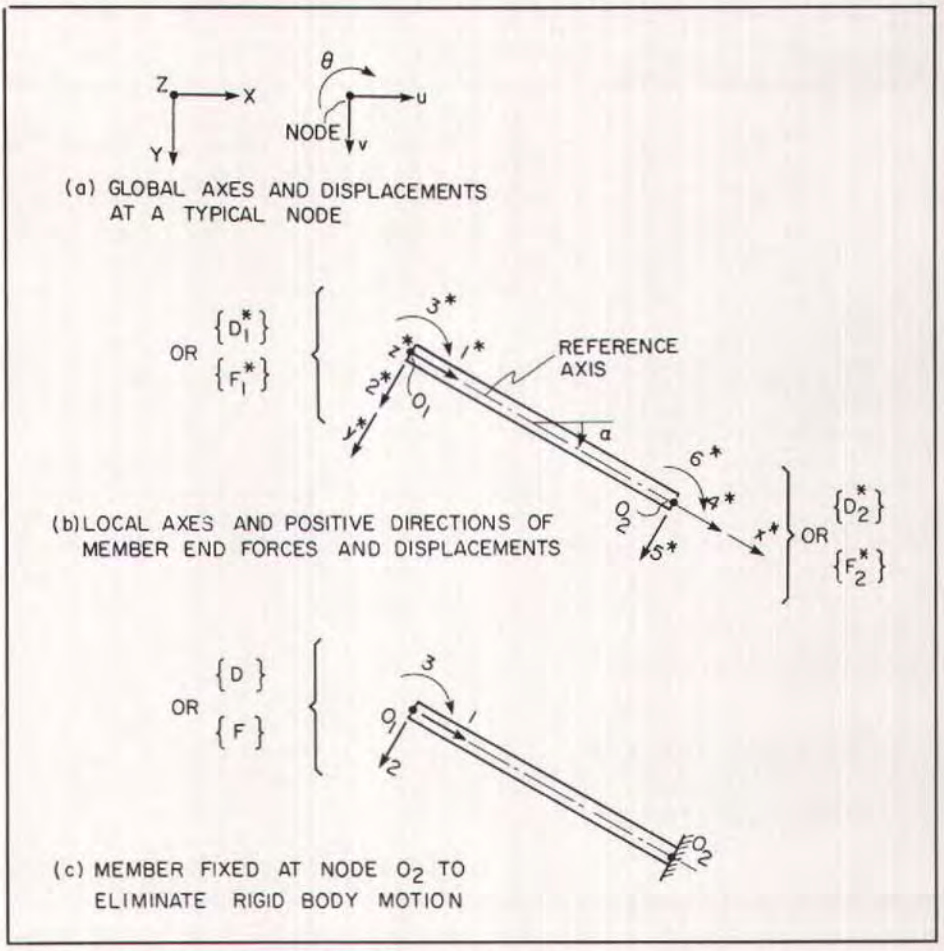

Fig. 3. Coordinate systems for plane frame analysis.

immediately before transfer. In case of post-tensioning, the jacking force is required as input data. Instantaneous losses due to friction and anchor set are calculated by:[15,16]

$$P_j = P_i e^{-(\mu \theta_{ij} + k s_{ij})} \quad (1)$$

$$\text{Area (ABC)} = \delta A_{ps} E_{ps} \quad (2)$$

where P_i and P_j are the prestressing forces at two consecutive sections, with section i closer to the jacking end; s_{ij} and θ_{ij} are, respectively, the length of the tendon and the change in its slope, in radians, between sections i and j; μ and k are the curvature and wobble friction coefficients, respectively. Values for μ and k are suggested in Refs. 17 and 18 for different types of tendons. Successive application of Eq. (1) starting from the jacking end gives the variation of the prestressing force along the tendon length as shown in Fig. 5.

When the anchor sets a distance δ, the jacking force drops and the friction force reverses direction over a length L_s. The shortening of the tendon over L_s is equal to δ.

This leads to Eq. (2) in which A_{ps} and E_{ps} are the cross-sectional area of the

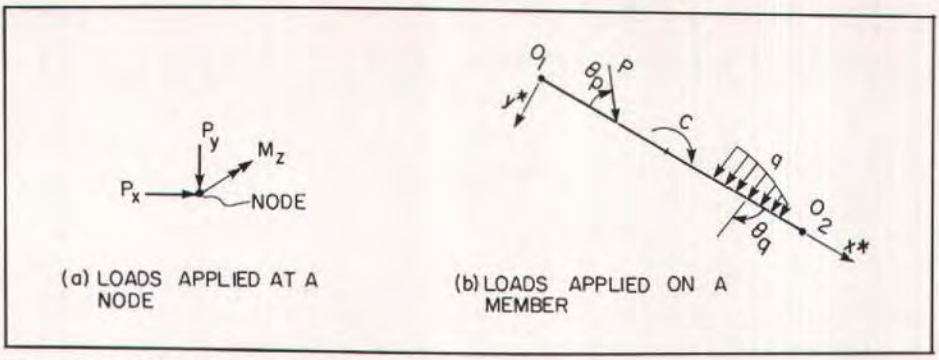

Fig. 4. External loads on a typical node or a member.

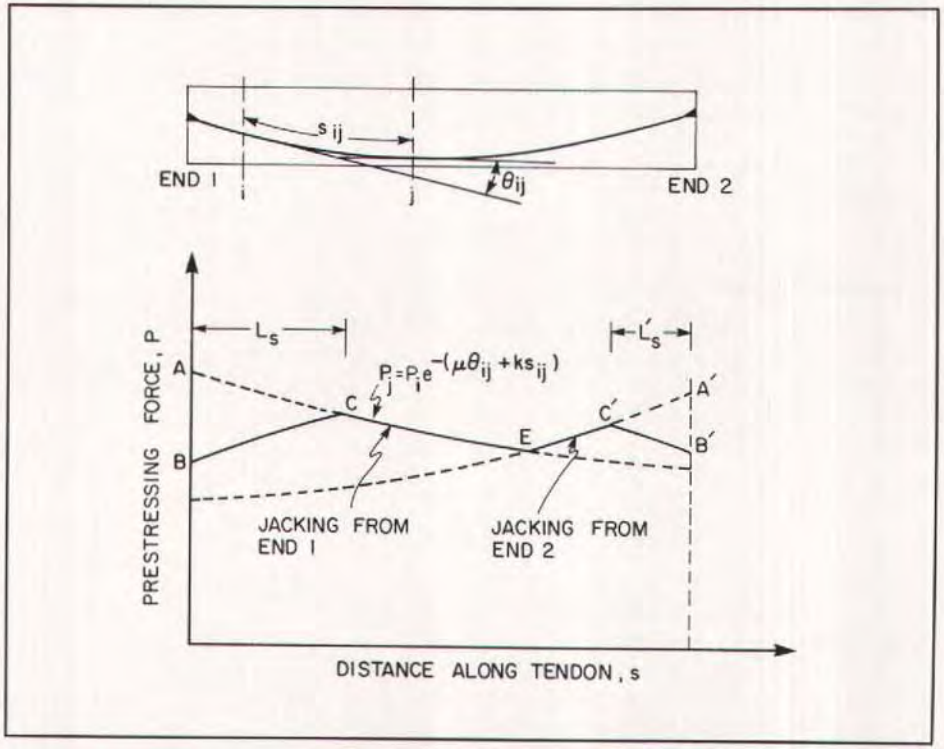

Fig. 5. Typical variation of prestressing force along a post-tensioned tendon after losses due to friction and anchor set (jacking from both ends).

tendon and its modulus of elasticity. In the computer program developed for the present study, Point C in Fig. 5 is determined by trial such that Eq. (2) is satisfied.

When jacking takes place at both ends, Eqs. (1) and (2) are applied measuring the parameters θ_{ij} and s_{ij} from each end, giving two values of P_j at each section; only the larger of the two values is of significance (curve BCEC'B' in Fig. 5).

ASSUMPTIONS AND CONSTITUTIVE RELATIONS

It is assumed that, under service loads, instantaneous strains and creep of concrete are linearly proportional to the applied stress. Steel reinforcements are also assumed to be within the elastic range. Plane cross sections before deformation are assumed to remain plane after deformation. Further, compatibility of strains is assumed between concrete and steel and between parts of composite cross sections.

Shrinkage of Concrete

The symbol $\Delta\epsilon_{cs}(t, t_0)$ represents the free (unrestrained) shrinkage of concrete during a period t_0 to t. In composite sections the value ϵ_{cs} can vary from part to part, but it is assumed to be constant over the cross-sectional area of any part.

Creep of Concrete

A stress increment $\Delta\sigma_c(t_0)$ introduced at time t_0 and sustained without change in magnitude up to time t produces instantaneous strain and creep of total magnitude:

$$\Delta\epsilon_c(t) = \frac{\Delta\sigma_c(t_0)}{E_c(t_0)}\,[1 + \phi(t, t_0)] \qquad (3)$$

where $E_c(t_0)$ is the modulus of elasticity of concrete at age t_0 and $\phi(t, t_0)$ is the creep coefficient.

When a stress increment $\Delta\sigma_c(t, t_0)$ is introduced gradually from zero at t_0 to its full value at t, the total strain at t will be:

$$\Delta\epsilon_c(t, t_0) = \frac{\Delta\sigma_c(t, t_0)}{\bar{E}_c(t, t_0)} \qquad (4)$$

where $\bar{E}_c$ is the age-adjusted modulus of elasticity of concrete:

$$\bar{E}_c(t, t_0) = \frac{E_c(t_0)}{1 + \chi\,\phi(t, t_0)} \qquad (5)$$

in which $\chi = \chi(t, t_0)$, the aging coefficient,[19,20] is usually between 0.6 and 0.9.

Suggested values of ϵ_{cs}, ϕ, χ and E_c, which are dependent upon the relative humidity, the size and shape of cross section and the age of concrete, are given in Refs. 12 and 20 to 23.

Step-by-Step Analysis

Let $t_1, t_2, \ldots$ represent instants at which external loads or prestressing are applied. The symbol $\Delta\sigma_c(t_j)$ will be used to represent a stress increment introduced at time t_j. In reinforced and prestressed concrete, the reinforcements restrain the deformations due to creep and shrinkage. The restraint subjects the concrete to stress increments which develop gradually. Let $\Delta\sigma_c(t_{j+1}, t_j)$ represent the stress increment gradually developed between t_j and t_{j+1}. In a later section, the analysis will be done step-by-step; for any interval i, the stress increments during earlier intervals will be known from the preceding calculations.

Assume that both $\Delta\sigma_c(t_j)$ and $\Delta\sigma_c(t_{j+1}, t_j)$ are known for $j = 1, 2, \ldots, i\text{-}1$. It is required to calculate the hypothetical free strain which would occur in the absence of the reinforcement during an interval t_i to t_{i+1}, with $i > j$. For this purpose, consider that $\Delta\sigma_c(t_j)$ and $\Delta\sigma_c(t_{j+1}, t_j)$ are lumped together as if the two increments occurred at t_j. Thus, the lumped stress increment produces creep during the interval considered equal to:

$$\frac{\Delta\sigma_c(t_j) + \Delta\sigma_c(t_{j+1}, t_j)}{E_c(t_j)} \times$$

$$[\phi(t_{i+1}, t_j) - \phi(t_i, t_j)]$$

If at t_i external loads are applied producing a stress $\Delta\sigma_c(t_i)$, the corresponding creep during the time t_i to t_{i+1} will be:

$$\frac{\Delta\sigma_c(t_i)}{E_c(t_i)}\,\phi(t_{i+1}, t_i)$$

Shrinkage during the same interval is

$\Delta\epsilon_{cs}(t_{i+1}, t_i)$. Thus, the total hypothetical free strain which would occur between t_i and t_{i+1} is given by:

$$\Delta\epsilon_c(t_{i+1}, t_i)_{free} = \sum_{j=1}^{i-1} \left\{ \frac{\Delta\sigma_c(t_j) + \Delta\sigma_c(t_{j+1}, t_j)}{E_c(t_j)} \times [\phi(t_{i+1}, t_j) - \phi(t_i, t_j)] \right\} + \frac{\Delta\sigma_c(t_i)}{E_c(t_i)} \phi(t_{i+1}, t_i) + \Delta\epsilon_{cs}(t_{i+1}, t_i) \quad (6)$$

Eq. (6) will later be used to derive the stresses developed in any time interval when the free strain in concrete is not free to occur due to the presence of the reinforcement or due to the attachment to other concrete parts having different creep or shrinkage parameters.

Relaxation of Prestressed Steel

The intrinsic relaxation, $\Delta\sigma_{pr}$, is the reduction with time in the stress of a prestressed tendon when it is stretched and held at a constant length between two fixed points.[24] The amount of intrinsic relaxation occuring during a given period of time depends to a great extent on the stress level in the steel.

In a prestressed concrete member, the prestressed steel commonly experiences a constantly dropping level of stress due to the effects of creep and shrinkage of concrete. Thus, the actual relaxation is expected to be smaller than the intrinsic value. Therefore, a reduced relaxation value $\Delta\bar{\sigma}_{pr}$ should be used in design. This reduced value equals the intrinsic relaxation multiplied by a reduction factor χ_r given by:[25]

$$\chi_r = e^{(-6.7+5.3\lambda)\Omega} \quad (7)$$

$$\Omega = -\frac{\Delta\sigma_{ps} - \Delta\sigma_{pr}}{\sigma_{p0}} \quad (8)$$

where λ is the ratio of the tensile stress σ_{p0} in the tendon at the start of the period considered to the tensile strength; $\Delta\sigma_{ps}$ is the change in stress in prestressed steel during the period considered due to the combined effects of creep, shrinkage and relaxation; and $\Delta\sigma_{pr}$ is the intrinsic relaxation in the same period. The value $\Delta\sigma_{ps}$ is generally not known a priori because it depends upon the reduced relaxation. Iteration is therefore necessary; first an assumed value $\chi_r = 0.7$ is used to calculate $\Delta\sigma_{ps}$ and later adjusted by Eq. (7).

Cracking of Concrete

The analysis is linear before cracking occurs. Nonlinearity occurs only when the stress in concrete exceeds its tensile strength, producing cracking. After cracking, concrete in tension is ignored and no tensile stresses can exist across the crack face. Only compressive stresses can develop across the crack face and a load reversal will cause reopening of the crack without any resistance.

In reality, tensile stresses exist in concrete between the root of the crack and the neutral axis. Also, between cracks, tensile stresses are transferred from the steel to the surrounding concrete by means of bond stresses. This enables concrete in the tension zone to contribute, to some extent, to the stiffness of the member, an effect which is usually referred to as the *tension stiffening effect* of concrete. This effect can be significant in members subjected to service load levels, and ignoring it can result in underestimation of stiffness and hence overestimation of displacements. Consideration of tension stiffening is discussed in a later section.

SIGN CONVENTION

Figs. 3 and 4 show the positive directions of the nodal displacements, of the member end forces and of the externally applied loads.

A tensile force, N, a tensile stress, σ,

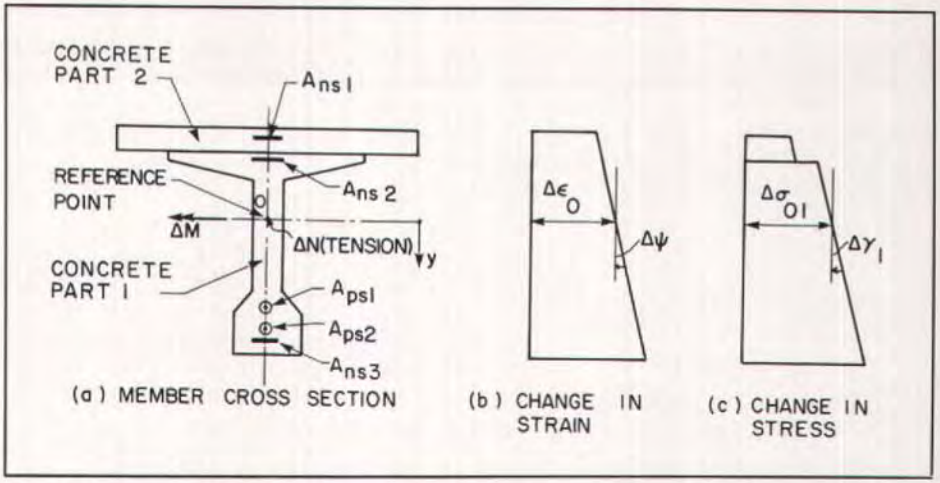

Fig. 6. Symbols and their positive sign convention.

and the corresponding strain, ϵ, are positive. A bending moment, M, is regarded as positive when producing tension at the bottom fiber. Positive curvature, ψ, and slope of stress diagram, γ, are associated with a positive moment (Fig. 6).

The reference axis O_1O_2 of a member (Fig. 3b) intersects any section at a reference point O. Any fiber below O has a positive y coordinate. The symbol Δ indicates a change in value; a positive Δ represents an increase. Thus, the symbols $\Delta\epsilon_{cs}$ and $\Delta\sigma_{pr}$ are always negative quantities.

INSTANTANEOUS STRESS AND STRAIN

Consider a composite cross section made up of concrete parts of different properties and reinforced with several prestressed and nonprestressed steel layers (Fig. 6a). At the start of any interval i, the cross section is subjected to increments of an axial force ΔN at an arbitrary reference point O and a bending moment ΔM.

The changes in stress and strain immediately after application of ΔN and ΔM can be determined by the equations given in Appendix A assuming that the composite section is replaced by a transformed section composed of the area of concrete in each part plus the area of the reinforcements, each multiplied by its modulus of elasticity and divided by an arbitrary reference value, E_{ref}.

The distribution of the strain change is assumed linear and is defined by the value $\Delta\epsilon_o$ at the reference point O and the slope $\Delta\psi$ (the curvature); see Fig. 6b. The two parameters can be determined from Eq. (A6). The stress distribution [Eq. (A2)] is in general represented by a separate straight line for each concrete part of the section; each line can be defined by two parameters: $\Delta\sigma_o$, the stress at O, and $\Delta\gamma$, the slope (Fig. 6c).

When construction is performed in stages, some concrete parts may not exist at a particular instant. Moreover, particularly in segmental construction, grouting of the prestressing ducts is carried out in stages or at the end of prestressing. To simplify input data, the sequence of grouting is ignored and it is assumed that grouting of an individual tendon is done shortly after its prestressing. When calculating the instan-

taneous changes in stress and strain at any stage, the properties of the transformed section exclude the areas of the nonexistent concrete parts and their reinforcement layers, and also the area of the ducts and the tendons which are prestressed at the stage considered or at later stages.

The equations in Appendix A are applicable to cracked and noncracked sections. The analysis of stresses and strains in a cracked section is discussed next.

STRESS AND STRAIN IN A CRACKED SECTION

Consider the strain and stress changes due to the effect of live load applied at time t producing at a composite cross section (Fig. 6a) a normal force ΔN at a reference point O and a bending moment ΔM. Assume that at time t prior to the application of ΔN and ΔM, the stress distribution is known and that it is defined by two values, $\sigma_o(t)$ and $\gamma(t)$, for each concrete part in the composite section (Fig. 6c). Assume that the magnitudes of ΔN and ΔM are high enough to produce cracking in concrete Part 1.

For the analysis of stresses and strains after cracking, partition ΔN and ΔM such that[12,14]

$$\left.\begin{aligned}\Delta N &= \Delta N_{decompression} + \Delta N_{fully\ cracked}\\ \Delta M &= \Delta M_{decompression} + \Delta M_{fully\ cracked}\end{aligned}\right\} \quad (9)$$

The pair $\{\Delta N,\ \Delta M\}_{decompression}$, referred to as the *decompression forces*, represents the forces which, when applied on the noncracked composite section, will bring the stresses in the concrete Part 1 to zero. The values $\{\Delta N,\ \Delta M\}_{decompression}$ are given by [Eq. (A5)]:

$$\left.\begin{aligned}\Delta N_{decompression} &= A(-\sigma_o)_1 + B(-\gamma)_1\\ \Delta M_{decompression} &= B(-\sigma_o)_1 + I(-\gamma)_1\end{aligned}\right\} (10)$$

where the subscript 1 refers to concrete Part 1; A, B and I are the area, and its first and second moments about an axis through the reference point O of the noncracked transformed section for which E_{ref} is $E_{c1}(t)$, the elasticity modulus of concrete of Part 1.

Under the effects of $\{\Delta N,\ \Delta M\}_{decompression}$ no cracking occurs and the changes in strain and stress at this stage can be determined by Eqs. (A6), (A1) and (A2) using the properties of the noncracked transformed section.

The forces $\{\Delta N,\ \Delta M\}_{fully\ cracked}$, which represent the portions of ΔN and ΔM in excess of the decompression forces, are applied on a transformed fully cracked section for which concrete in tension is ignored. Eqs. (A6), (A1) and (A2) can again be applied to determine the changes in strain and stress due to $\{\Delta N,\ \Delta M\}_{fully\ cracked}$. The transformed section properties A, B and I to be used in this stage must include only the area of concrete in the compression zone plus the area of reinforcements. Thus, the depth c of the compression zone (Fig. B1b) must be determined before A, B and I can be calculated. Determination of the depth c is discussed in Appendix B.

The total change in strain and stress due to ΔN and ΔM is the sum of the values calculated for the decompression and the cracking stages.

In the composite section considered in Fig. 6a, it is unlikely that, under service conditions, cracking will extend beyond the full height of concrete Part 1. For this reason, ΔN and ΔM are partitioned in Eq. (9) into two portions only. In a more general case, when cracking of the two concrete parts occurs, an additional portion of ΔN and ΔM necessary for decompression of concrete in Part 2 must be determined before application of $\{\Delta N,\ \Delta M\}_{fully\ cracked}$ on the fully cracked section. For further details of cracking in composite sections, the reader can see Ref. 14.

In the next section, time-dependent stresses and strains will be considered first for noncracked sections and then for cracked sections.

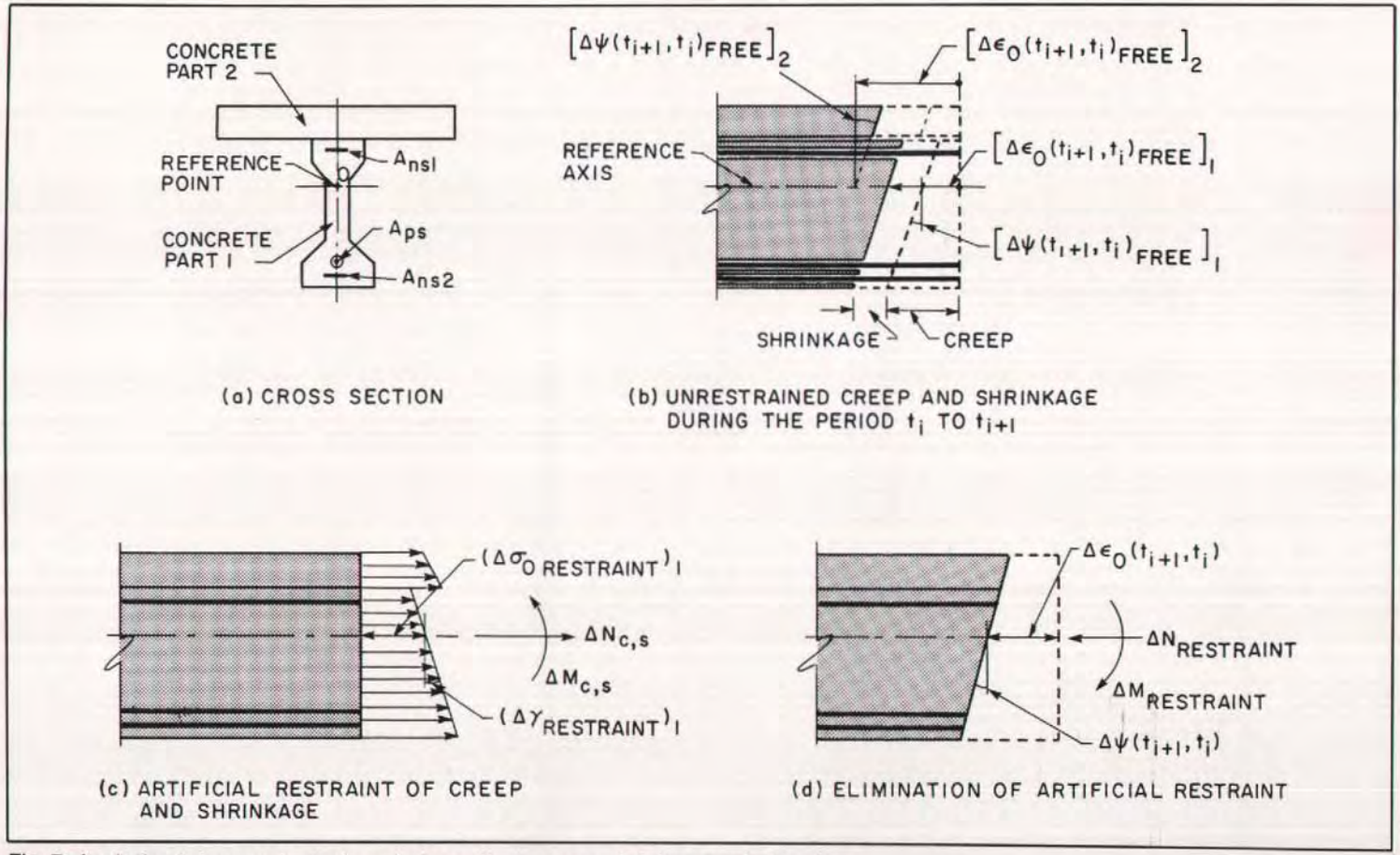

Fig. 7. Analysis of changes in strain and stress due to creep, shrinkage and relaxation.

TIME-DEPENDENT STRESSES AND STRAINS

Noncracked Sections

Consider a composite section (Fig. 7a) for which the distribution of the hypothetical free strain due to creep and shrinkage during a period t_i to t_{i+1} has been determined [Eq. (6)]. Thus, two parameters are known defining the strain distribution over each concrete part (Fig. 7b): $[\Delta\epsilon_o(t_{i+1}, t_i), \Delta\psi(t_{i+1}, t_i)]_{free}$. The curvature $\Delta\psi(t_{i+1}, t_i)_{free}$ can be determined by Eq. (6) by replacing σ with γ $(= d\sigma/dy)$, the slope of stress diagram, and setting $\epsilon_{cs} = 0$.

It is required to determine the time-dependent changes in stress and strain occurring in each concrete part between time t_i and t_{i+1}, assuming the material parameters ϕ, χ, ϵ_{cs} and $\Delta\bar{\sigma}_{pr}$ are known for the time interval considered.

In Fig. 7c, the hypothetical free strain can be prevented by introducing an artificial stress whose distribution over the jth concrete part is defined by a stress value at O and the slope:

$$(\Delta\sigma_{O\ restraint})_j = -[\bar{E}_c\,\Delta\epsilon_O(t_{i+1}, t_i)_{free}]_j \tag{11}$$

$$(\Delta\gamma_{restraint})_j = -[\bar{E}_c\,\Delta\psi(t_{i+1}, t_i)_{free}]_j \tag{12}$$

where $\bar{E}_{cj} = [\bar{E}_c(t_{i+1}, t_i)]_j$ is the age-adjusted modulus of elasticity of concrete Part j [Eq. (5)].

The forces $\Delta N_{c,s}$ and $\Delta M_{c,s}$ shown in Fig. 7c represent the resultants of the artificial stress. The values of these forces can be determined by [Eq. (A5)]:

$$\Delta N_{c,s} = \sum_{j=1}^{m}(A_c\,\Delta\sigma_{O\ restraint} + B_c\,\Delta\gamma_{restraint})_j \tag{13}$$

$$\Delta M_{c,s} = \sum_{j=1}^{m}(B_c\,\Delta\sigma_{O\ restraint} + I_c\,\Delta\gamma_{restraint})_j \tag{14}$$

The summations in these equations are performed for the concrete parts. For each part A_c, B_c and I_c are the concrete cross-section area, and its first and second moments about an axis through O.

The strain in concrete due to relaxation of prestressed steel can be artificially prevented by applying the forces:

$$\Delta N_{pr} = \sum_{k=1}^{n}(\Delta\bar{\sigma}_{pr}A_{ps})_k \tag{15}$$

$$\Delta M_{pr} = \sum_{k=1}^{n}(\Delta\bar{\sigma}_{pr}A_{ps}y_{ps})_k \tag{16}$$

where the summations are performed for the prestressed steel layers tensioned before or at t_i. A_{psk} and y_{psk} are the cross-sectional area and the y coordinate of the kth prestressed steel layer.

Summing up the forces in Eqs. (13) to (16) gives $\{\Delta N, \Delta M\}_{restraint}$, the total forces which would artificially prevent creep, shrinkage and relaxation.

The artificial restraint is eliminated by the application of $\{\Delta N, \Delta M\}_{restraint}$ in reversed directions on the age-adjusted transformed section (Fig. 7d). This produces the change in strain $\Delta\epsilon(t_{i+1}, t_i)$ defined by the value at O, $\Delta\epsilon_O(t_{i+1}, t_i)$, and the slope of the strain diagram, $\Delta\psi(t_{i+1}, t_i)$; see Fig. 7d. These two parameters can be calculated by Eq. (A6) using the properties of the age-adjusted transformed section: E_{ref}, $\bar{A}$, $\bar{B}$ and $\bar{I}$. The age-adjusted transformed section is composed of the area of concrete in each part, multiplied by $\bar{E}_c/E_{ref}$, plus the area of reinforcements, multiplied by E_s/E_{ref}.

Multiplication of the strain shown in Fig. 7d by $\bar{E}_c$ of each concrete part gives the corresponding stress change. The sum of this stress and the stress in Fig. 7c gives the total stress increment, $\Delta\sigma_c(t_{i+1}, t_i)$.

Cracked Sections

The analysis of the time-dependent strain and stress increments presented earlier applies also to cracked sections

in which the concrete in tension is ignored. The transformed section is composed only of the concrete in compression and the reinforcements. Appendix B gives the equations from which the depth $c(t_i)$ of the compression zone is determined due to any specified combination of normal force and moment applied at time t_i. The normal force and moment used here should be equal to the increments introduced at t_i minus the decompression forces discussed in the preceding section [Eq. (9)].

Due to creep and shrinkage during the period t_i to t_{i+1}, the depth c gradually changes and the new value $c(t_{i+1})$ can be determined by iteration:

1. Perform the time-dependent analysis presented earlier, ignoring the change in c. The depth of the area of concrete taken into account in determining the properties of the transformed section is $c(t_i)$. The analysis gives the stress distribution at time t_{i+1} and hence a new value $c(t_{i+1})$.

2. Repeat the calculations using $c(t_i)$ when determining the artificial forces necessary to restrain creep, while using $c(t_{i+1})$ for the remainder of the calculations. This will give a new stress distribution and a new $c(t_{i+1})$. If this value is substantially different from the value previously determined, this step is repeated. Usually one or two iterations are sufficient.

It can be shown, however, that if the depth c of the effective area of concrete is assumed constant between t_i and t_{i+1}, while allowing the neutral axis position to change with time, a small error results in the time-dependent changes in strain (see discussion of Ref. 13). The error is small because an area of concrete close to the neutral axis is ignored, although it is subjected to compressive stresses.

The iteration procedure discussed in Steps 1 and 2 is included in the computer program CPF;[26] hence, the effect of change in c on the stiffness of members and on the statically indeterminate internal forces is not ignored.

MEAN STRAIN AND CRACK WIDTH

Displacements of a member can be calculated by integration of the axial strain and the curvature determined at a number of sections along the member length. For a cracked member, displacements can be evaluated more accurately if the concrete in tension is not completely ignored (i.e., if the tension stiffening effect of concrete is taken into account). One way of doing this is to use mean values of axial strain and curvature determined by interpolation between two limiting states: the state with concrete area assumed fully effective (noncracked) and the state in which concrete in tension is ignored. The following empirical interpolation equation[22,23] is adopted here:

$$\left.\begin{aligned} \epsilon_{0\,mean} &= (1-\zeta)\,\epsilon_{0\,noncracked} + \zeta\,\epsilon_{0\,fully\,cracked} \\ \psi_{mean} &= (1-\zeta)\,\psi_{noncracked} + \zeta\,\psi_{fully\,cracked} \end{aligned}\right\} \quad (17)$$

The interpolation coefficient ζ is given by:

$$\zeta = 1 - \beta_1 \beta_2 \left(\frac{f_{ct}}{\sigma_{max}}\right)^2 \quad (\text{with } \zeta \geq 0.4) \quad (18)$$

where f_{ct} is the tensile strength of concrete; σ_{max} is the hypothetical stress at the extreme tension fiber that would exist after application of the load assuming no cracking; $\beta_1 = 1$ or 0.5 for high bond or plain reinforcing bars, respectively; $\beta_2 = 1$ for the first loading and equals 0.5 for loading applied in a sustained manner or in large number of cycles.

Assuming that cracks are spaced at a distance s, the mean value of crack width at the level of a steel layer is:

$$w = \zeta s\, \Delta\epsilon_{s\,fully\,cracked} \quad (19)$$

where $\Delta\epsilon_{s\,fully\,cracked}$ is the change in steel strain calculated for a fully cracked sec-

tion. Empirical equations are available[23] to predict the crack spacing s. Here it is assumed that s is given as input data.

The parameter ζ represents the extent of cracking and the damage of bond after occurrence of cracks. The value of ζ approaches unity as the internal forces increase above the values causing first cracking. Once cracking has occurred at a section, it will remain cracked for any subsequent loading even when the internal forces drop below the values which produced the first cracking. Also, the parameter ζ will continue to assume the highest value reached under earlier loadings.

STIFFNESS MATRIX OF A MEMBER

In the preceding sections, equations were presented to calculate the changes in axial strain and curvature in non-cracked and cracked sections due to forces applied on the section or due to the effects of creep, shrinkage and relaxation. In the present and following sections, the changes in axial strain and curvature will be used in the analysis of the corresponding changes in internal forces of statically indeterminate plane frames.

The typical plane frame member shown in Fig. 3b has six degrees of freedom located at the two end nodes O_1 and O_2. Fix the member at end O_2 (Fig. 3c) and generate a flexibility matrix $[f]$ corresponding to the three coordinates at end O_1. The elements in any column j of the matrix $[f]$ are:

$$f_{1j} = -\int_0^l \epsilon_{oj}\,dx; \qquad f_{2j} = -\int_0^l \psi_j x\,dx;$$

$$f_{3j} = \int_0^l \psi_j\,dx \tag{20}$$

where ϵ_{oj} and ψ_j are the strain at the reference axis O_1O_2 and the curvature produced at any section at distance x from O_1 by a unit force applied at coordinate j, with $j = 1, 2$ or 3.

The integrals in Eq. (20) are evaluated numerically employing values of ϵ_o and ψ determined at a number of sections using Eq. (A6). For analysis of instantaneous effects, use the modulus of elasticity of concrete and the transformed section properties at the time of application of the load. When the analysis is for the time-dependent changes during a period t_i to t_{i+1}, the age-adjusted elasticity modulus $\bar{E}_c(t_{i+1}, t_i)$ and the properties of the age-adjusted transformed section are to be used to give the age-adjusted flexibility, $[\bar{f}]$.

After cracking, the flexibility of a cracked member is obtained by replacing ϵ_o and ψ in Eq. (20) with mean values $\epsilon_{o\,mean}$ and ψ_{mean} determined from Eq. (17). This requires that the depth c of the compression zone and the interpolation coefficient ζ be known a priori. An iterative procedure will therefore be necessary (to be discussed in a separate section).

Inversion of $[f]$ gives a 3 x 3 stiffness matrix corresponding to the coordinates at O_1 (Fig. 3c). The forces at end O_2 (Fig. 3b) are obtained by equilibrium and thus the stiffness matrix for the six coordinates is generated:

$$[S] = [H]^T[f]^{-1}[H] \tag{21}$$

where

$$[H] = \begin{bmatrix} 1 & 0 & 0 & -1 & 0 & 0 \\ 0 & 1 & 0 & 0 & -1 & l \\ 0 & 0 & 1 & 0 & 0 & -1 \end{bmatrix}$$

with l being the length of the member.

FIXED-END FORCES

For external loads applied at any position between the two ends of a member (Fig. 4b), the fixed-end forces at the three coordinates at end O_1 (Fig. 3c) are:

$$\{\Delta F\} = -[f]^{-1}\{\Delta D\} \tag{22}$$

where $\{\Delta D\}$ represents the three dis-

placements at end O_1 with the member treated as a cantilever (Fig. 3c) and subjected to the given loads. Corresponding axial strain and curvature determined by Eq. (A6) are to be used to calculate $\{\Delta D\}$:

$$\Delta D_1 = -\int_0^l \Delta\epsilon_o\, dx;$$

$$\Delta D_2 = -\int_0^l \Delta\psi x\, dx;$$

$$\Delta D_3 = \int_0^l \Delta\psi\, dx \qquad (23)$$

For a cracked section, $\Delta\epsilon_{o\ mean}$ and $\Delta\psi_{mean}$ are to be used in Eq. (23) instead of $\Delta\epsilon_o$ and $\Delta\psi$, and the values of c and ζ must be known from earlier steps of analysis. The forces at end O_2 can be determined by equilibrium, and thus, the six fixed-end forces (Fig. 3b) can be expressed as:

$$\{\Delta F^*\} = [H]^T\{\Delta F\} + \{\Delta R\} \qquad (24)$$

The first three elements in vector $\{\Delta R\}$ are zero, while the last three are the three reactions due to external loads applied on a cantilever fixed at end O_2 (Fig. 3c).

To determine the time-dependent changes in the fixed-end forces during an interval t_i to t_{i+1}, calculate for the cantilever the increments $\Delta\epsilon_o\ (t_{i+1}, t_i)$ and $\Delta\psi\ (t_{i+1}, t_i)$. These values are substituted in Eq. (23) to give the time-dependent displacement increments $\{\Delta D\ (t_{i+1}, t_i)\}$.

Substitution in Eq. (22), replacing $[f]$ with $[\bar{f}]$, gives the changes in the fixed-end forces $\{\Delta F\ (t_{i+1}, t_i)\}$ at end O_1. These are substituted in Eq. (24), with $\{\Delta R\} = \{0\}$, to give the increments $\{F^*\ (t_{i+1}, t_i)\}$ of the six fixed-end forces at the two ends.

ANALYSIS PROCEDURE

For each time interval, the conventional displacement method of analysis[11] is employed to determine the changes in displacements, reactions and internal forces which occur instantaneously at the beginning of the interval due to application of loads or prestressing and to calculate the time-dependent changes due to creep, shrinkage and relaxation.

The displacements at the nodes, the internal forces, the stresses and the strains at various sections existing before introduction of new loads, or at the beginning of any interval, are assumed known. If cracking has occurred at any section, the values c and ζ are also known. At the beginning of the analysis, before application of any loads, all of these variables are zero except c, which equals the full depth of the section.

For each construction stage, load application or time interval, the analysis is performed in steps:

1. Generate the stiffness matrix for individual members. Calculate the relative end displacements $\{\Delta D\}$ and the fixed-end forces $\{\Delta F^*\}$ [see Figs. 3b and c and Eqs. (22) to (24)]. The values of c and ζ, needed in the calculation of axial strain and curvature at any section, are those existing prior to application of the new loads. Assemble the fixed-end forces and apply in a reversed direction on the structure, and then determine by a conventional linear analysis the increments of nodal displacements and internal forces. When the analysis is for time-dependent changes, the stiffness to be used in this step is the age-adjusted stiffness.

2. Add the increments of nodal displacements and internal forces to the existing values. Compute the changes in axial strain, curvature, and stresses, accounting for any cracking, at all sections. Add the changes in strain and stress to the existing values. Update c and ζ.

3. Use the current axial strain and curvature to calculate the relative end displacements $\{D\}$ of individual members using Eq. (23). The same displacements can be calculated by:

$$\{D\} = [H]\{D^*\} \quad (25)$$

where $\{D^*\}$ are the nodal displacements at the member ends (Fig. 3b). When cracking does not occur, the relative end displacements by the two methods will be equal. When this is not the case, calculate the difference in displacements and substitute in Eqs. (22) and (24) to obtain a vector of residual fixed-end forces. Note that for these calculations $\{\Delta R\} = \{0\}$ in Eq. (24) and $[f]$ is based on the updated c and ζ values.

4. The residual forces calculated in Step 3 for the individual members are assembled and applied in a reversed direction to the structure with its stiffness updated. Determine by a conventional analysis the increments in nodal displacements and in internal forces.

5. Go back to Step 2 and terminate the analysis if the residual forces calculated in Step 3 are smaller than prescribed values or when the increments in nodal displacements are less than a specified percentage of the current total values.

It is worth noting that this analysis has an advantage over the standard finite element techniques, particularly when nonprismatic members are involved. The essential feature of the present analysis is that the actual deflected shape of a member is obtained by integration of the actual strains and curvatures.

In the finite element method, the deflected shape of a member is usually assumed as a function of the displacements at the nodes, and equilibrium between the external and the internal forces is satisfied only at the nodes. A larger number of elements is usually needed to overcome this drawback, especially in those places where a markedly nonlinear behavior is expected.

A computer program will greatly facilitate the preceding analytical steps and evaluation of the equations. This is described next.

COMPUTER PROGRAM

A computer program, CPF (Cracked Plane Frames in Prestressed Concrete),[26] has been developed to perform the analysis presented here. The program gives the instantaneous values and the time-dependent changes in joint displacements, support reactions and internal forces, stresses and strains in concrete and steel, and the crack width at selected sections.

CPF is suitable for the analysis of structures composed of precast or cast-in-place segments or of members cast and erected at different ages. The difference in the time-dependent deformations of the parts is accounted for when the members have different ages or when the cross sections of individual members are composed of concrete parts of different ages.

The logic of the CPF program is illustrated in the flow chart in Fig. 8. The program requires a small core storage and can be used on a microcomputer.

To demonstrate the applicability of the present method of analysis, the CPF program is employed for the analysis of two bridge examples presented in the following section. Further details and results on these and other examples are given in Ref. 27.

APPLICATIONS

EXAMPLE 1

Fig. 9 shows a three-span symmetrical bridge made of a steel box and concrete deck. The deck is made of precast rectangular segments; each segment has the full width of the deck and covers a short part of the span. The segments are post-tensioned longitudinally as shown in Fig. 9a. Dimensions and area properties of the cross section are given in Fig. 9b and Table 1. The example borrows most of its dimensions from the design of Arvid Grant and Associates of the Wallace Viaduct in Idaho.

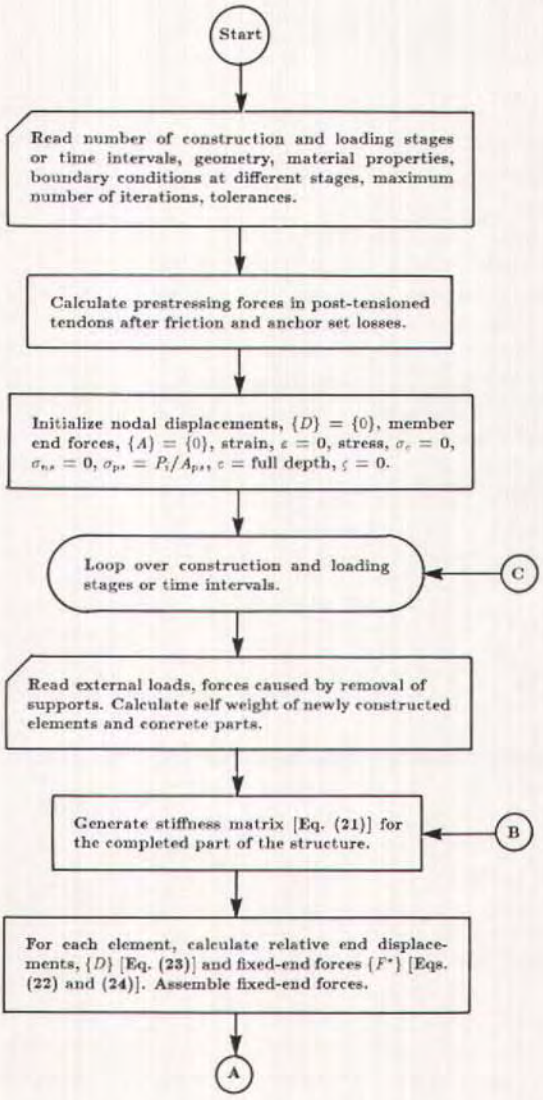

Fig. 8. Flow chart for computer program CPF.

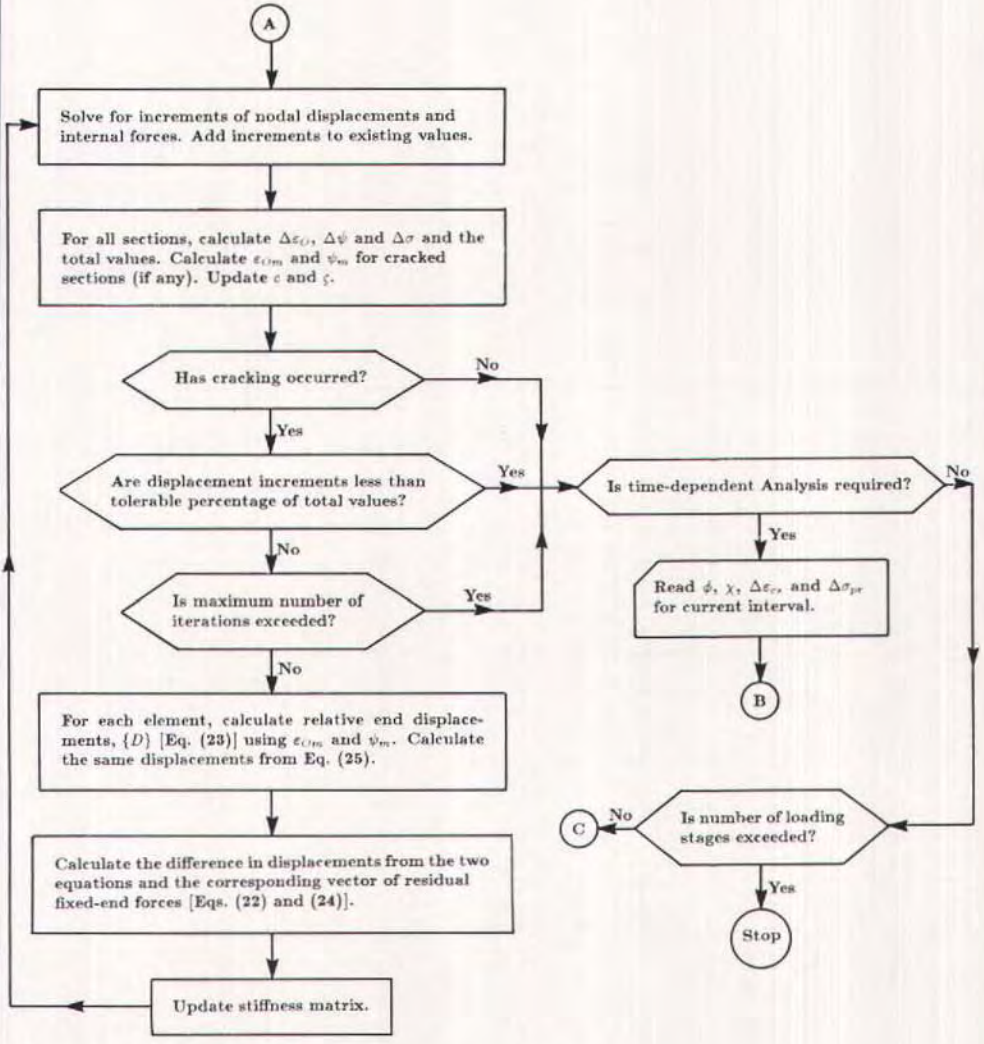

Fig. 8 (cont). Flow chart for computer program CPF.

Table 1. Variation of cross section properties over bridge length (Example 1).

Section	Region	A	B	C
Steel box	Top flange thickness (in.)	2¼	1⅛	¾
	Bottom flange thickness (in.)	2	1¼	⅞
	Web plate thickness (in.)	9/16	9/16	7/16
	Cross-sectional area (in.²)	279	190	124
	Centroid above bottom (in.)	32	29.5	25
	Moment of inertia about centroid (in.⁴)	248,000	146,000	81,500
Concrete deck	Gross cross-sectional area (in.²)	4,372	4,500	4,543
	Centroid above bottom (in.)	9.5	10.34	10.61
	Gross moment of inertia about centroid (in.⁴)	85,500	98,100	102,800

Note: 1 in. = 25.4 mm; 1 in.² = 645.2 mm²; 1 in.⁴ = 416231 mm⁴.

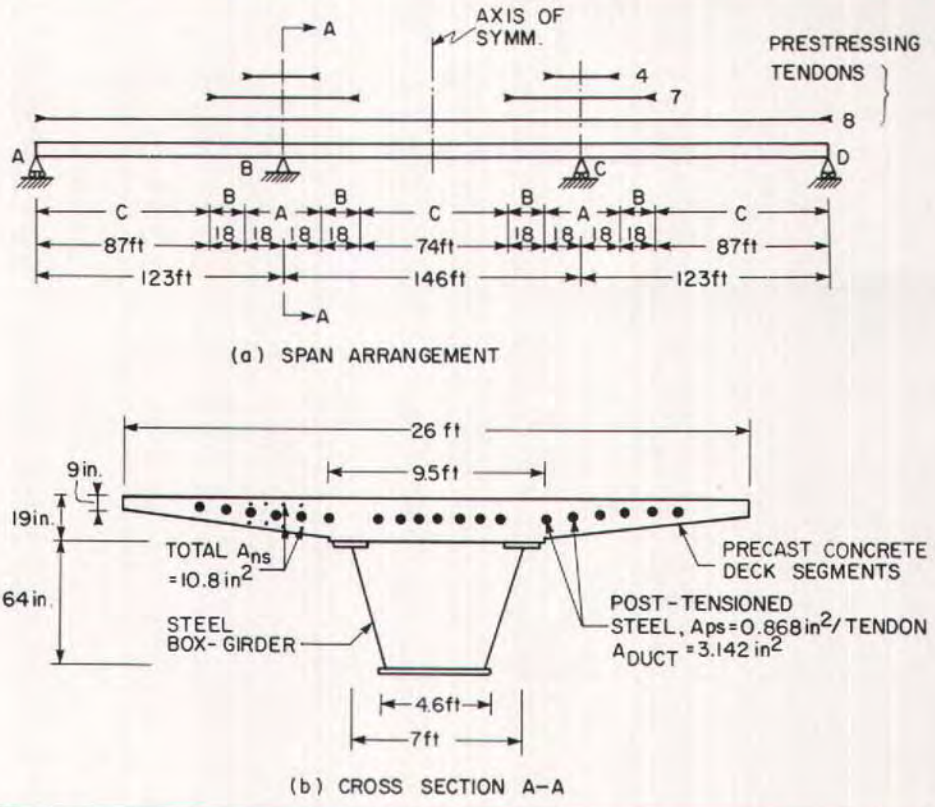

Fig. 9. Three-span composite concrete-steel bridge (Example 1). Note: 1 in. = 25.4 mm; 1 in.² = 645.2 mm²; 1 ft = 0.3048 m.

The construction is performed in the following sequence: The steel girder is placed in position without shoring to carry a load of 4.3 kips/ft (62.7 kN/m), representing its own weight and the weight of the precast concrete segments which is introduced in steps. First, segments are placed in Region A (Fig. 9a) and post-tensioned with four tendons. Segments are then added in Region B and post-tensioned from end to end using seven tendons. The bridge deck is completed by placing segments in Region C and post-tensioning eight tendons throughout the bridge length.

The precast segments are of age 60 days at the time of post-tensioning and the prestressing force per tendon is 164 kips (730 kN). Shortly after prestressing, the bridge is made composite by casting concrete to fill in pockets in the precast segments at the location of studs welded to the top flanges of the steel girder. Finally, 30 days after erection of the steel girder, a superimposed dead load of 0.4 kip/ft (5.8 kN/m), representing the surface cover, is applied and the bridge is opened to traffic.

Because of the advanced age of the precast segments and the short period of construction, the time-dependent changes in stress and strain are calculated for the time interval $t = 60$ to $t = \infty$, and the self weight and the superimposed dead load are applied at $t = 60$ and sustained thereafter.

Other data are: $E_s = E_{ns} = 29{,}000$ ksi (200 GPa); $E_{ps} = 27{,}000$ ksi (186 GPa); $E_c(60) = 3200$ ksi (22 GPa); $\phi(\infty, 60) = 2.28$; $\chi = 0.788$; $\Delta\epsilon_{cs}(\infty, 60) = -230 \times 10^{-6}$; $\Delta\bar{\sigma}_{pr}(\infty, 60) = -13$ ksi (-90 MPa.) Friction is ignored here for simplicity but is considered in Example 2.

For comparison, the analysis is performed with the steel girder unshored (as described above) and repeated for shored construction. The shores are assumed closely spaced and removed immediately after the structure becomes composite. Some results for the unshored and shored constructions are given in Figs. 10 through 13. The results represent the effects of self weight, superimposed dead load and prestressing.

The restraint provided by the steel girder and the prestressed and nonprestressed steels to the time-dependent deformations of the concrete deck produces important changes in internal forces. Fig. 10a shows the variation over half the bridge length of the bending moments immediately after completion of construction and at time $t = \infty$. The bending moment at any section is here considered as the resultant of the stresses on all components: the steel box, the nonprestressed and prestressed reinforcements, and the concrete.

The variations of the tensile force in the prestressed tendons at the time of prestressing and at time infinity are plotted in Fig. 10b.

The deflected shapes of the bridge at completion of construction and at $t = \infty$ are depicted in Fig. 11. As expected, shoring during construction reduces deflection considerably, and the time-dependent changes in deflection are larger in shored than in unshored constructions.

The stress distribution at two critical sections are given at completion of construction and at $t = \infty$ in Figs. 12 and 13 for unshored and shored constructions, respectively. A substantial reduction in the compressive stresses produced by prestressing in the deck slab occurs due to time-dependent effects. For example, the average stress in the slab is changed over the interior support from -675 to -175 psi (-4.7 to -1.2 MPa) (see Fig. 12).

It can be noted that the small loss in tension in the tendons (Fig. 10b) has no practical significance because it does not represent loss of compression in the concrete. It can also be seen from Figs. 12 and 13 that the time-dependent change in stress in the steel box is mainly compression; an increase of 6,000 to 12,000 psi (41.4 to 82.8 MPa)

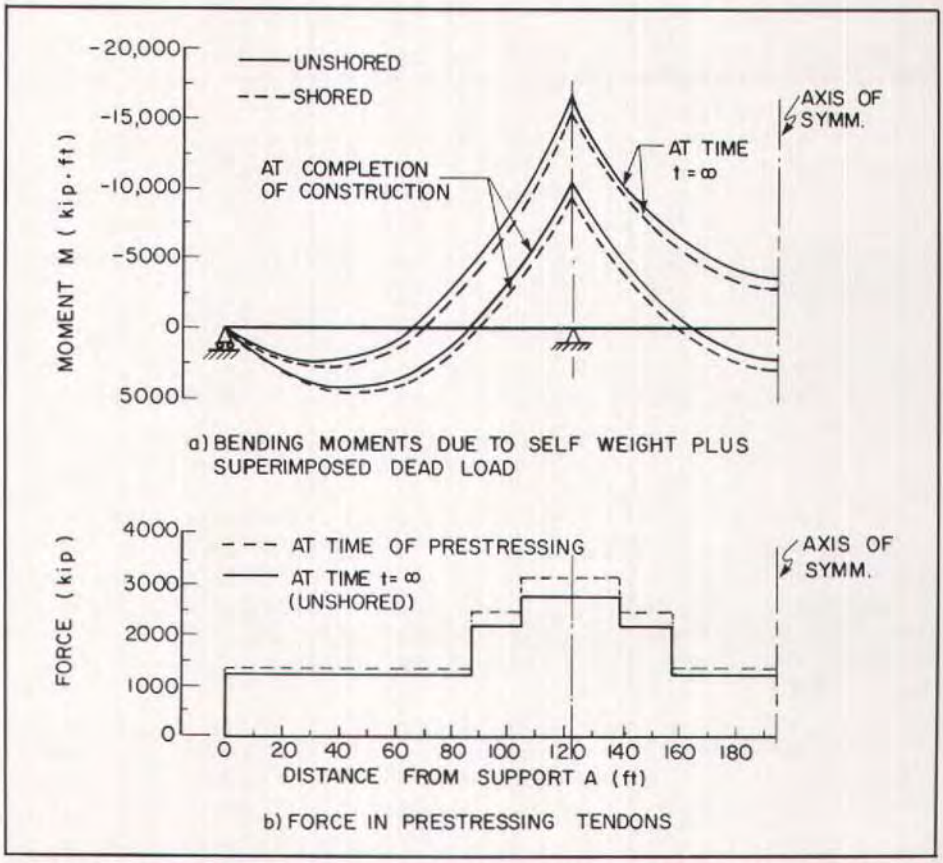

Fig. 10. Variation of bending moments and force in prestressing tendons in the bridge of Example 1. Note: 1 ft = 0.3048 m; 1 kip = 4.448 kN; 1 kip-ft = 1.356 kN•m.

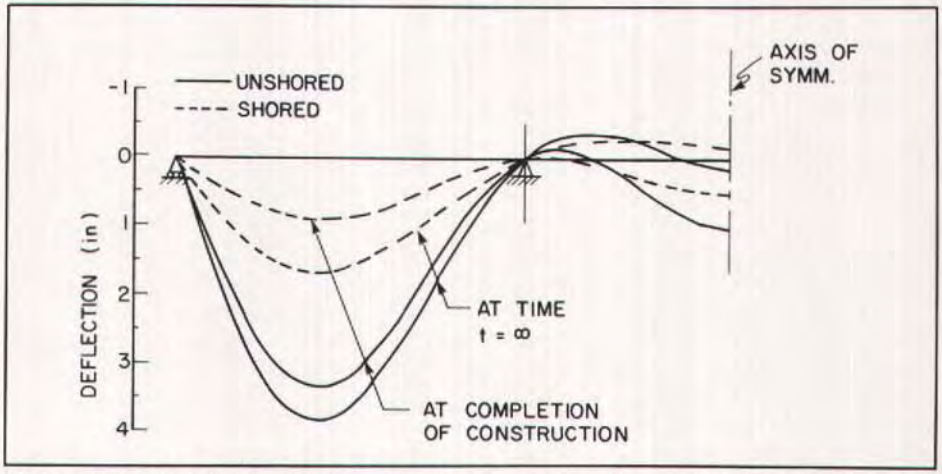

Fig. 11. Deflected shapes of half the length of the bridge of Example 1 due to self weight plus superimposed dead load. Note: 1 in. = 25.4 mm.

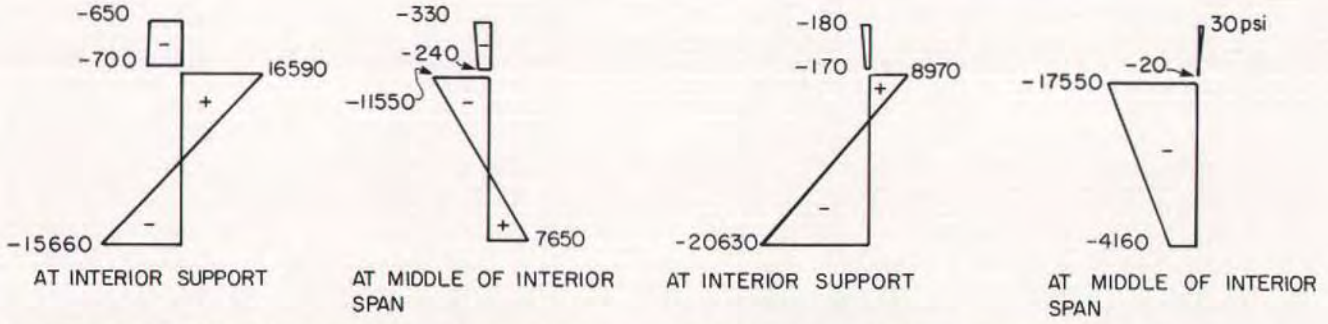

Fig. 12. Stress distributions at critical sections — unshored construction. Note: 1 psi = 6.895 × 10^{-3} MPa.

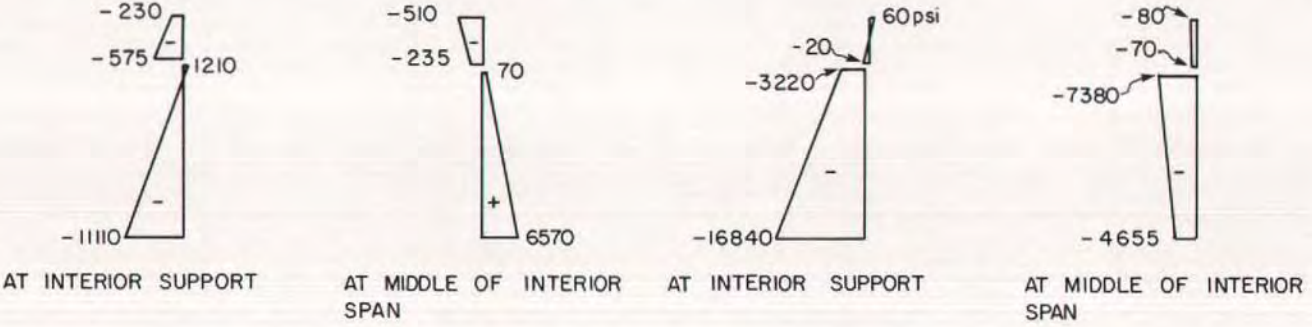

Fig. 13. Stress distributions at critical sections — shored construction. Note: 1 psi = 6.895 × 10^{-3} MPa.

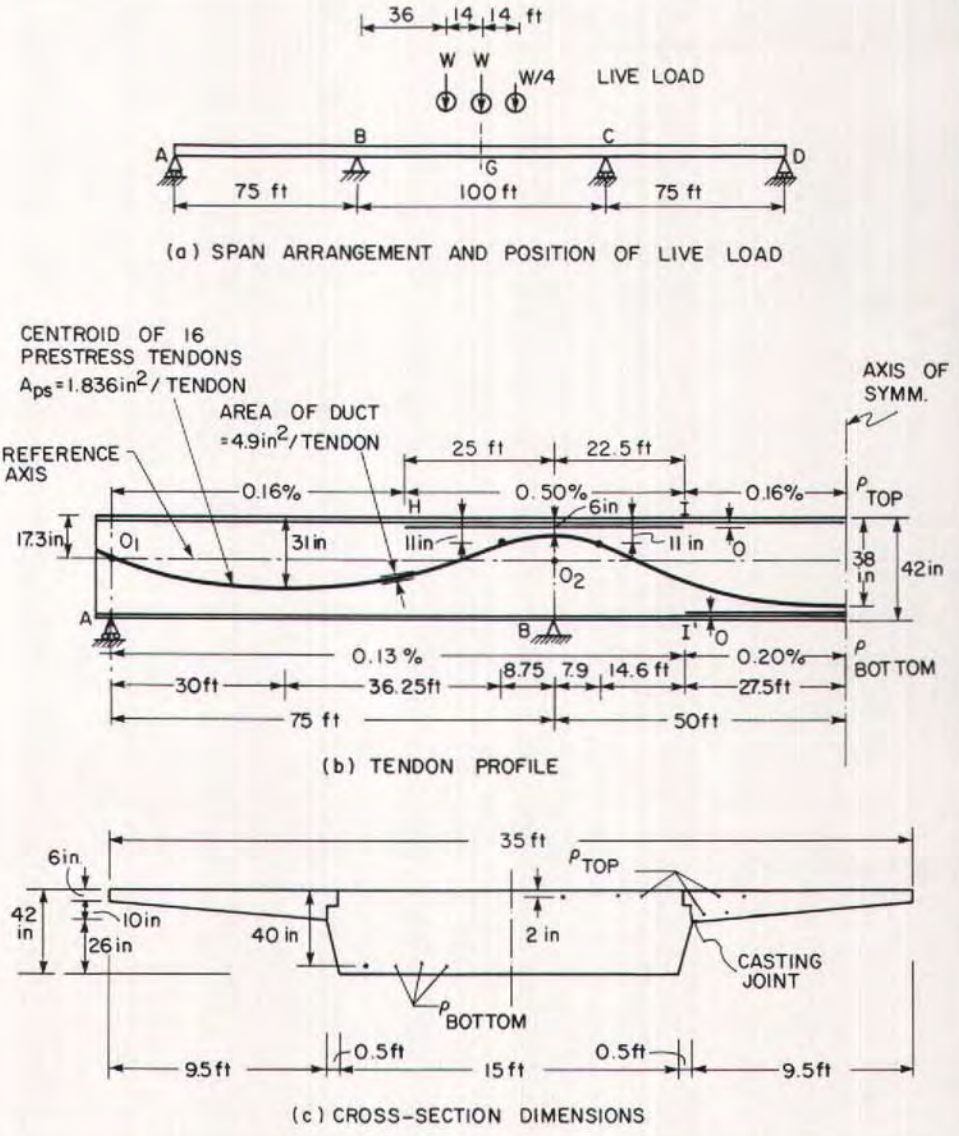

Fig. 14. Three-span concrete bridge cast and prestressed in stages (Example 2). Note: 1 in. = 25.4 mm; 1 in.^{2} = 645.2 mm^2; 1 ft = 0.3048 m.

can be seen at various locations. Recall that the analysis assumes no slip between the concrete and the steel; the increase in compression on the steel would be smaller if slip occurs.

EXAMPLE 2

The computer program CPF is employed also for the analysis of the partially prestressed three-span continuous bridge shown in Fig. 14. The bridge

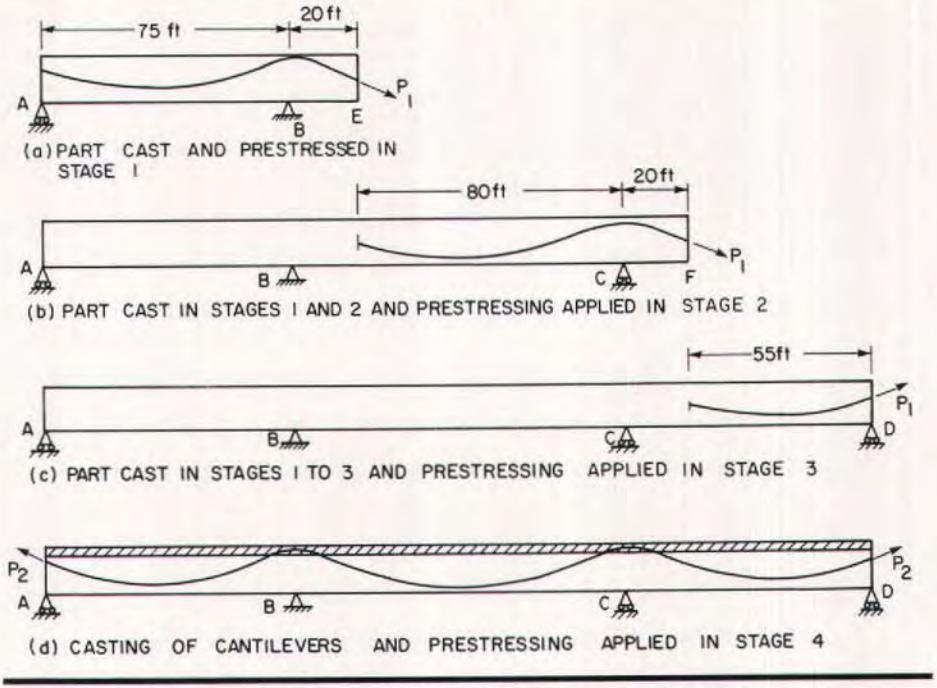

Fig. 15. Construction and prestressing stages of the bridge of Example 2.
Note: 1 ft = 0.3048 m.

cross section is made of a solid slab of 3.5 ft (1.05 m) depth, with two side cantilevers providing a two-lane roadway (Fig. 14c). The bridge is post-tensioned with 16 tendons having the profile shown in Fig. 14b; each tendon consists of twelve ½ in. strands. The span arrangement and the concrete dimensions of the cross section are adopted from those reported in Ref. 28.

Here the bridge is assumed to be built in the following stages (Fig. 15). At time $t = 0$, the thicker part of the deck of width 16 ft (4.8 m) (referred to as the *spine*) is cast over a length AE covering Span AB and 20 ft (6 m) overhang (Fig. 15a). At $t = 14$ days, the same part AE is prestressed with 11 longitudinal tendons (P_1) and its forms are removed.

Twenty-eight days later, the spine is completed for the remainder of Span BC and 20 ft (6 m) of Span CD. Prestressing P_1 is applied on this part at $t = 56$ days (Fig. 15b). The remaining portion of the spine in Span CD is cast at $t = 84$ days and prestressed with P_1 at $t = 98$ days (Fig. 15c).

The completed spine serves as a track carrying a moving carriage for forming and casting of the two cantilevered parts of the deck in the period $t = 98$ to 126 days. During the same period, five additional longitudinal tendons (P_2) are prestressed (Fig. 15d). To simplify the analysis, the application of the weight of the cantilevers and the prestressing P_2 are lumped as if they occurred in one instant at $t = 126$ days. Transverse tendons are required to join the cantilevers to the spine. However, their effects are not included in the present analysis. The superimposed dead load of the wearing surface, curbs, etc., is introduced at $t = 154$ days.

Table 2. Time-dependent properties of concrete in the bridge of Example 2.

Construction and loading stages	Time		Spine in Part ABE				Cantilevers			
	t_i	t_j	$E_c(t_i)$ ksi	$\phi(t_j,t_i)$	$\chi(t_j,t_i)$	$\epsilon_{cs}(t_j,t_i)$ 10^{-6}	$E_c(t_i)$ ksi	$\phi(t_j,t_i)$	$\chi(t_j,t_i)$	$\epsilon_{cs}(t_j,t_i)$ 10^{-6}
Stage 1	14	56	4500	0.88	0.85	−13				
	14	98		1.19						
	14	126		1.32						
	14	154		1.43						
	14	10000		3.21						
Stage 2	56	98	5017	0.57	0.90	−12				
	56	126		0.77						
	56	154		0.91						
	56	10000		2.93						
Stage 3	98	126	5106	0.36	0.91	−7				
	98	154		0.57						
	98	10000		2.70						
Stage 4	126	154	5134	0.33	0.95	−7	4500	0.91	0.83	−42
	126	10000		2.58				3.59		
Superimposed dead load	154	10000	5151	2.48	0.78	−300	4950	3.25	0.79	−371
Live load	10000	10000	5232				5232			

Note: $t = 0$ at the day of casting of the spine in part ABE; 1 ksi = 6.895 MPa.

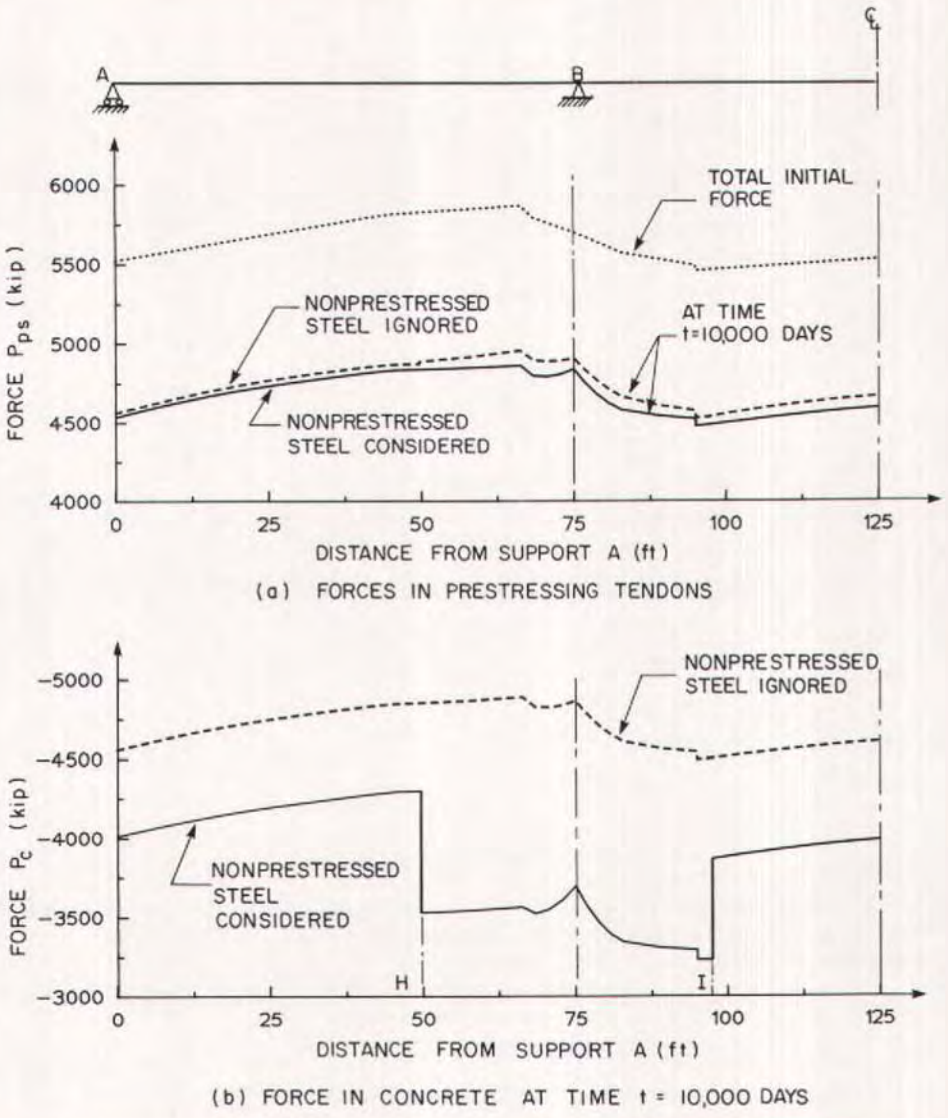

Fig. 16. Forces in prestressing tendons and in concrete after time-dependent losses. Note: 1 ft = 0.3048 m; 1 kip = 4.448 kN.

The dead loads are: self weight of spine = 8.2 kips/ft (120 kN/m); weight of cantilevers = 2.6 kips/ft (38 kN/m); superimposed dead load = 1.65 kips/ft (24 kN/m). The prestressing force at the time of jacking = 390 kips (1735 kN) per tendon. A live load representing a truck is applied at the position shown in Fig. 14a at time t = 10,000 days.

The spine and the cantilevers are assumed to be made of the same concrete; however, the parameters E_c, ϕ, χ and ϵ_{cs}

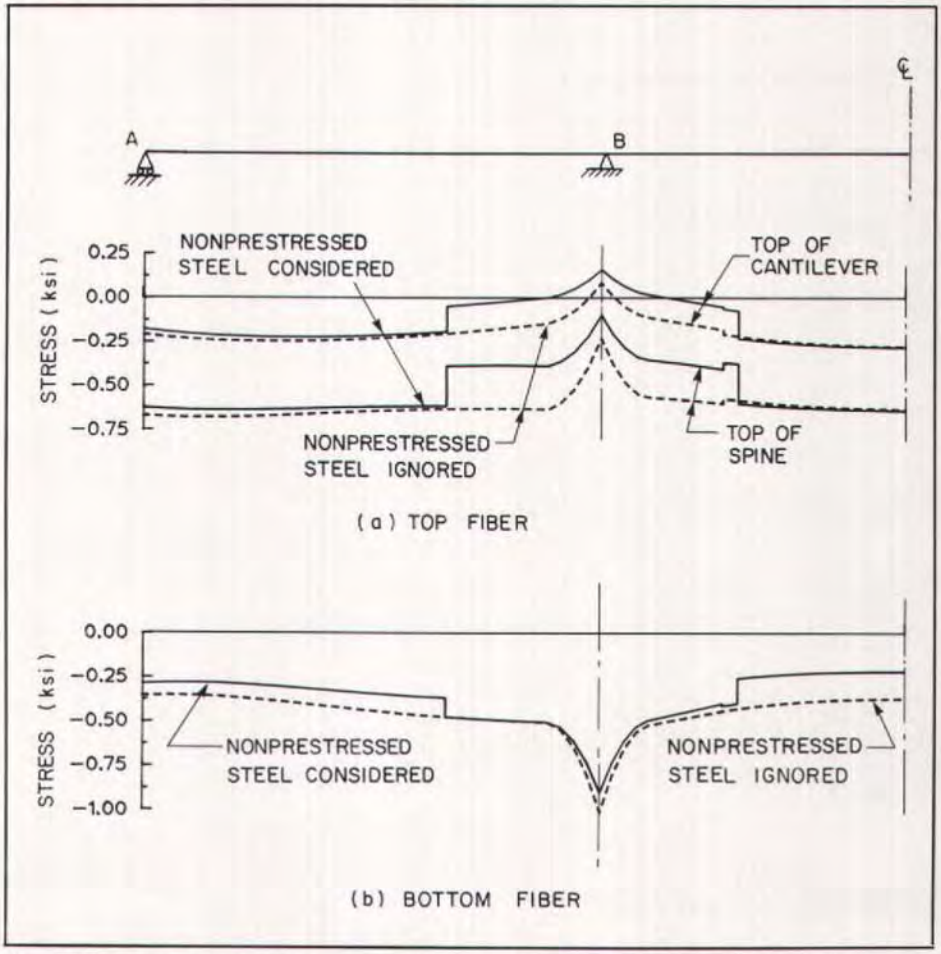

Fig. 17. Concrete stresses at top and bottom fibers at t = 10,000 days just before application of live load. Note: 1 ksi = 6.895 MPa.

differ according to the age. These are taken according to the CEB Model Code;[22] for brevity, Table 2 gives the parameters only for the spine in Part ABE and for the cantilevers.

Other material properties are: f_{ct} = 0.35 ksi (2.4 MPa); E_{ns} = 29,000 ksi (200 GPa); E_{ps} = 27,500 ksi (190 GPa); $\beta_1 = 1$ and $\beta_2 = 0.5$; curvature friction coefficient, μ = 0.15/radian; wobble coefficient, $k = 7.5 \times 10^{-4}$/ft (2.5×10^{-3}/m); anchor slip, δ = 0.2 in. (5 mm). The intrinsic relaxation at time infinity, $\Delta\sigma_{pr\infty} = -25$ ksi (−172 MPa); values for shorter periods are calculated from Eqs. (4) to (6) of Ref. 25; the relaxation reduction factor, χ_r = 0.7. The nonprestressed reinforcements near the top and bottom fibers are indicated in Fig. 14b as percentages of the cross section area.

Two analyses are performed, one with the nonprestressed steel considered and the other with the presence of this steel ignored. Figs. 16 through 21 present some results of the two analyses. Although the bridge is not symmetrical under the effects of prestressing and live load, results are presented only for the

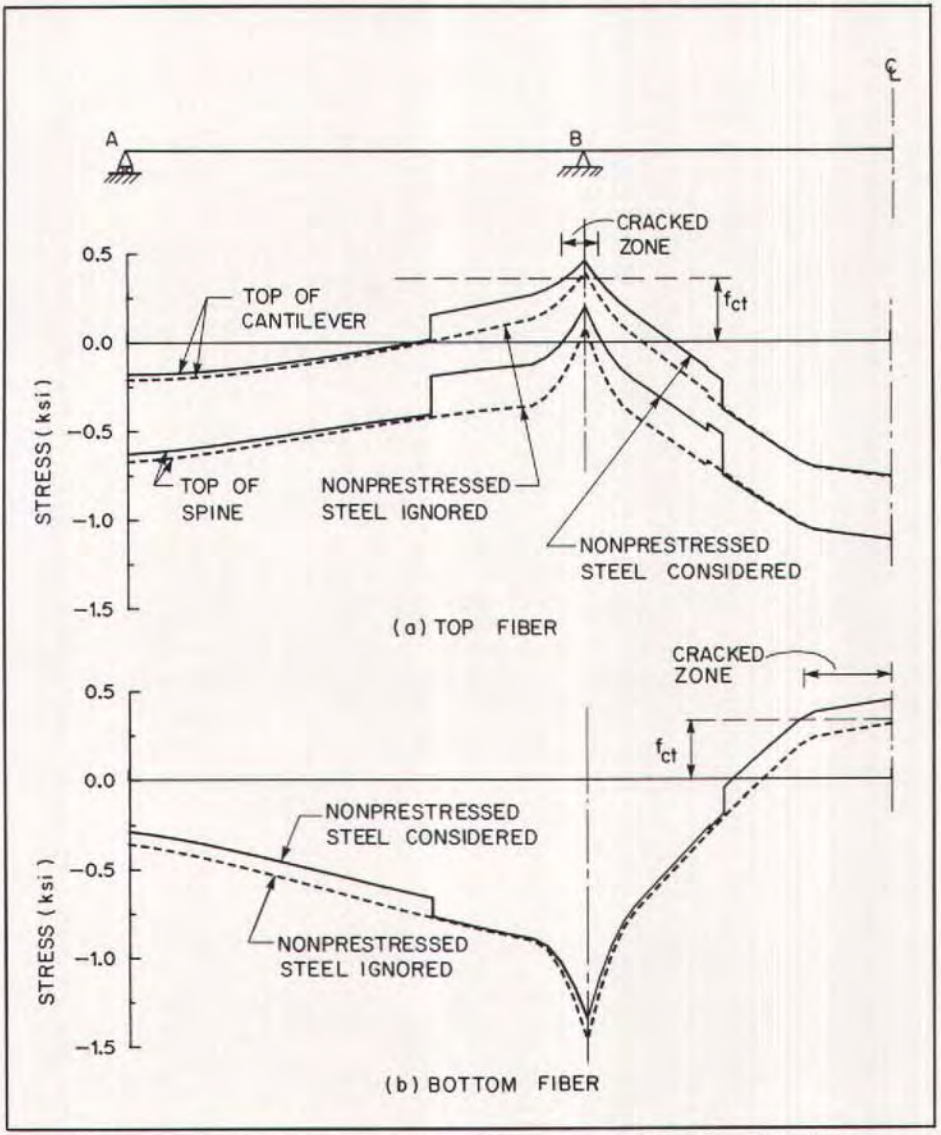

Fig. 18. Concrete stresses at top and bottom fibers at t = 10,000 days just after application of live load, W = 130 kips (578 kN). Note: 1 ksi = 6.895 MPa.

half of the bridge length which experiences larger stresses and deformations.

The variations of the total prestressing force in all tendons after the friction losses and after the time-dependent losses are shown in Fig. 16a. As shown, presence of nonprestressed steel results in a small reduction in the loss of tension in the prestressed steel. However, the loss in tension is not equal in absolute value to the loss of compression in the concrete. In fact, in the presence of nonprestressed steel, a large compressive force is gradually transmitted from the concrete to this reinforcement, resulting in a much larger loss in compres-

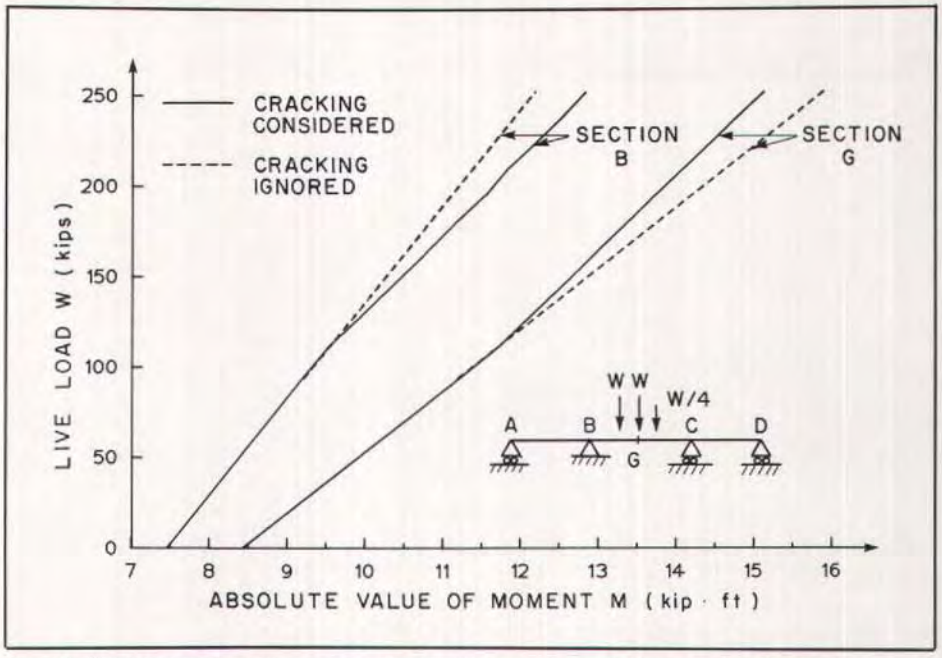

Fig. 19. Variation of bending moments at critical sections with increasing live load.
Note: 1 kip = 4.448 kN; 1 kip-ft = 1.356 kN•m.

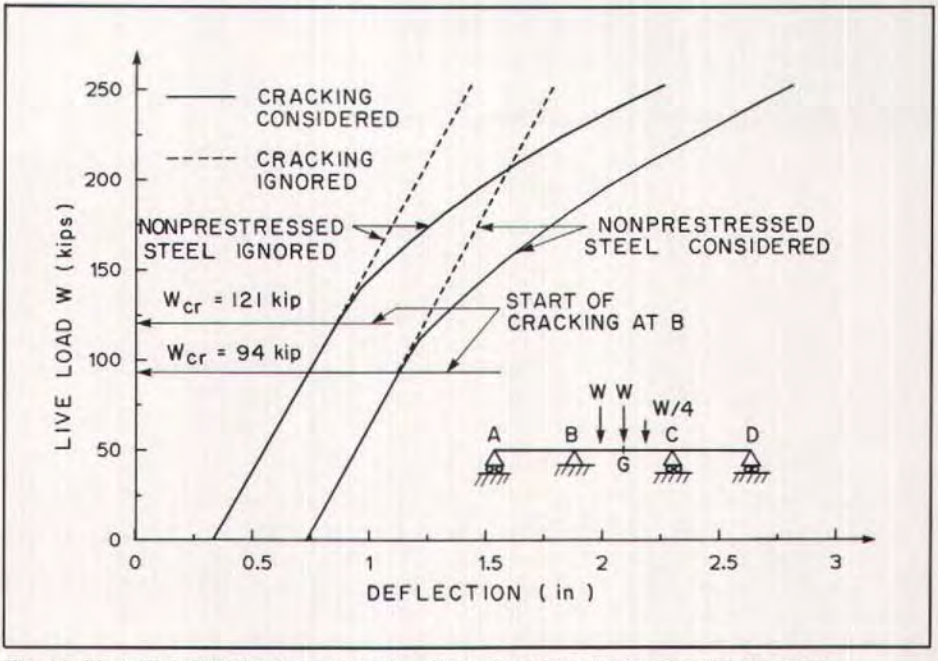

Fig. 20. Variation of deflection at middle of interior span with increasing live load.
Note: 1 in. = 25.4 mm; 1 kip = 4.448 kN.

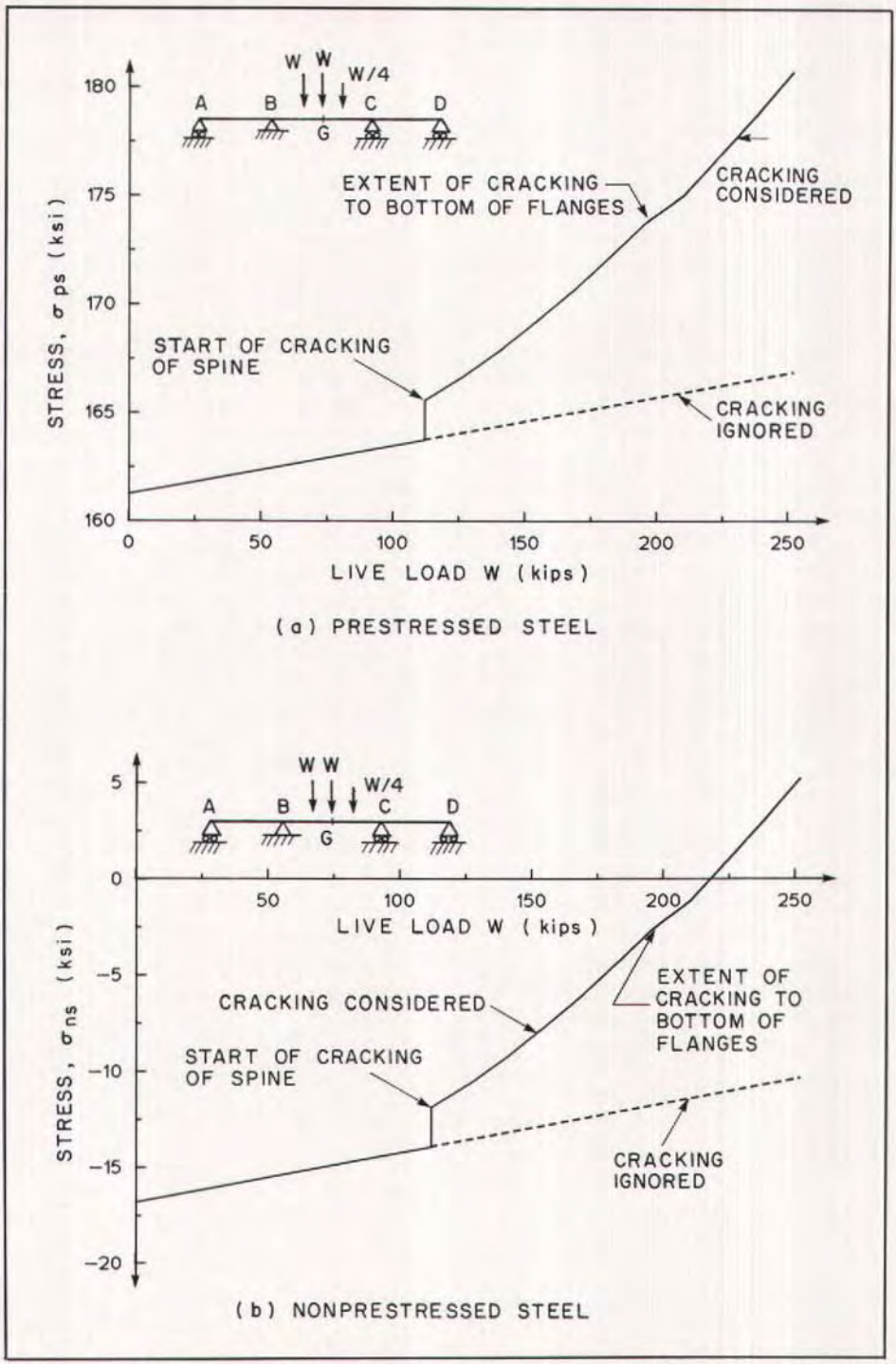

Fig. 21. Steel stresses at Section G, middle of interior span: variation with increasing live load. Note: 1 kip = 4.448 kN; 1 ksi = 6.895 MPa.

sion on the concrete. This is shown in Fig. 16b, which represents the variation of the resultant compressive force in concrete at t = 10,000 days. The difference in the ordinates between the two curves in Fig. 16b represents the compression in the nonprestressed steel. The two steps in the continuous curve at H and I in Fig. 16b are due to the curtailments of the nonprestressed steel (see Fig. 14b).

The variation of concrete stresses at the top and bottom fibers just before and after application of live load with W = 130 kips (578 kN) (Fig. 14a) is depicted in Figs. 17 and 18, respectively. Fig. 18 shows the zones in which the tensile strength of concrete (f_{ct} = 0.35 ksi) is exceeded, indicating cracking. Where cracking occurs, Program CPF recalculates the stress distribution over the section, ignoring the concrete in tension, and determines the mean values of axial strain and curvature accounting for the tension stiffening [Eqs. (17) and (18)]. Fig. 18 represents the stress variation before the concrete in tension is ignored.

The dashed lines in Figs. 17 and 18 represent the stresses when the presence of nonprestressed steel is ignored. The analysis based on this assumption would indicate no cracking while, in fact, cracking occurs over almost 30 percent of the length of the interior span.

The graphs in Figs. 19 through 21 represent, respectively, the variation with increasing live load, W, of the bending moment at two critical sections, and the deflection and the stresses in the prestressed and nonprestressed steels at the middle of the interior span.

The dashed lines in Figs. 19 through 21 illustrate the case of a linear analysis which ignores cracking, while the continuous lines are for the analysis which accounts for cracking. As shown, there is a substantial difference between the results of the two analyses.

Fig. 20 indicates that ignoring the presence of nonprestressed steel results in an underestimation of the deflection at the middle of the interior span and an overestimation of the live load level at which cracking occurs [W_{cr} = 121 kips (538 kN) instead of 94 kips (418 kN)].

For the stresses in the prestressed and nonprestressed steels, Figs. 21a and b show that when the live load produces cracking a large increase in stress occurs. This increase in stress can be important if fatigue is of concern. Also, the increment in stress in the nonprestressed steel at and after cracking can be used to predict the width of cracks.

For the cracked section at the middle of the interior span and for a live load W = 250 kips (1112 kN), the analysis gives $\Delta\epsilon_{s\ fully\ cracked} = 735 \times 10^{-6}$ for the bottom nonprestressed steel and ζ = 0.93 [Eq. (18)]. Assuming a mean crack spacing, s = 1 ft (0.3 m), Eq. (19) gives a mean value for the crack width, w = 0.008 in. (0.2 mm).

* * *

SUMMARY AND CONCLUSION

A numerical procedure based on the displacement method is presented for the serviceability analysis of reinforced concrete plane frames with or without prestressing. The analysis accounts for the effects of friction and anchor setting, creep and shrinkage of concrete and relaxation of prestressed steel, and for the effects of cracking on the stresses and deformations.

Variation of concrete properties within individual cross sections and from one member to another is taken into account. External loads and prestressing can be applied in stages. Prestressing can be of any magnitude varying from zero, allowing cracking, to full prestressing, eliminating cracks. The effect of cracking on the reactions and internal forces in statically indeterminate frames is analyzed by an iterative procedure. Equilibrium of forces and compatibility of strains in the prestressed and nonprestressed steels and in the concrete are used to calculate time-dependent variations of the forces in the three components. The need for use of empirical equations for prediction of prestress losses is eliminated.

The procedure is implemented in an available computer program which is suitable for the analysis of a wide range of frames including continuous bridges built span by span, segmental construction, and structures built of precast prestressed concrete members connected and made continuous by cast-in-place concrete deck or joints and a second stage prestressing. The program can also be used for the analysis of multistory structures which are generally constructed in several stages.

The program gives the instantaneous and time-dependent changes in the displacements, the reactions and statically indeterminate forces and the corresponding stresses and strains, and the crack widths at various sections. The program requires a small core storage and can be used on a microcomputer.*

Two bridge examples are presented to show the significance of the time-dependent deformations and cracking on the serviceability of a composite steel bridge and a partially prestressed concrete bridge built in stages.

*A version of CPF on diskette, for use on IBM microcomputers, is available from the Civil Engineering Department, The University of Calgary, 2500 University Drive N.W., Calgary, Alberta, Canada T2N 1N4.

* * *

ACKNOWLEDGMENT

The research work reported in this paper was financially supported by an Izaak Walton Killam Memorial Scholarship and a grant from the Natural Sciences and Engineering Research Council of Canada which are greatly appreciated. Grateful appreciation is also due to Arvid Grant and Associates, Olympia, Washington, for providing the data for the bridge in Example 1.

REFERENCES

1. Brown, R. C., Jr., and Burns, N. H., "Computer Analysis of Segmentally Erected Bridges," *Journal of the Structural Division*, American Society of Civil Engineers, V 101, No. ST4, April 1975, pp. 761-778.
2. Danon, J. R., and Gamble, W. L., *Time-Dependent Deformations and Losses in Concrete Bridges Built by the Cantilever Method*, Structural Research Series No. 437, Civil Engineering Studies, University of Illinois at Urbana-Champaign, Urbana, Illinois, 1977, 169 pp.
3. EEG, *B.C. Bridge Construction Computer Program Manual*, Europe Etudes Gecti, Paris, France, 1977.
4. Tadros, M. K., Ghali, A., and Dilger, W. H., "Long-Term Stresses and Deformations of Segmental Bridges," PCI JOURNAL, V. 24, No. 4, July-August 1979, pp. 66-87.
5. Khalil, M. S. A., "Time-Dependent Non-Linear Analysis of Prestressed Concrete Cable-Stayed Girders and Other Concrete Structures," PhD Thesis, Department of Civil Engineering, The University of Calgary, Calgary, Alberta, Canada, April 1979, 246 pp.
6. Van Zyl, S. F., and Scordelis, A. C., "Analysis of Curved Prestressed Segmental Bridges," *Journal of the Structural Division*, American Society of Civil Engineers, V. 105, No. ST11, November 1979, pp. 2399-2417.
7. Marshall, V., and Gamble, W. L., *Time-Dependent Deformations in Segmental Prestressed Concrete Bridges*, Structural Research Series No. 495, Civil Engineering Studies, University of Illinois at Urbana-Champaign, Urbana, Illinois, 1981.
8. Shushkewich, K. W., "Time-Dependent Analysis of Segmental Bridges," *Computer and Structures*, V. 23, No. 1, 1986, pp. 95-118.
9. Ketchum, M. A., "Redistribution of Stresses in Segmentally Erected Prestressed Concrete Bridges," Report No. UCB/SESM-86/07, Structural Engineering and Structural Mechanics, University of California at Berkeley, Berkeley, California, May 1986, 238 pp.
10. Elbadry, M. M., and Ghali, A., "Design of Concrete Bridges for Temperature Variations," presented at ACI Symposium on "Serviceability Criteria and Concern for Bridges" at the ACI Annual Convention in Seattle, Washington, November 1987.
11. Ghali, A., and Neville, A. M., *Structural Analysis: A Unified Classical and Matrix Approach*, Second Edition, Chapman and Hall, London, England, 1978, 779 pp.
12. Ghali, A., and Favre, R., *Concrete Structures: Stresses and Deformations*, Chapman and Hall, London and New York, 1986, 352 pp.
13. Ghali, A., "A Unified Approach for Serviceability Design of Prestressed and Nonprestressed Reinforced Concrete Structures," PCI JOURNAL, V. 31, No. 2, March-April, 1986, pp. 118-137. See also discussion, V. 32, No. 1, January-February 1987, pp. 133-140.
14. Ghali, A., and Elbadry, M. M., "Cracking of Composite Prestressed Concrete Sections," *Canadian Journal of Civil Engineering*, V. 14, No. 3, June 1987, pp. 314-319.
15. Naaman, A. E., *Prestressed Concrete Analysis and Design – Fundamentals*, McGraw Hill Book Co., New York, N.Y., 1982, 670 pp.
16. Huang, T., "Anchorage Take-up Loss in Post-tensioned Members," PCI JOURNAL, V. 14, No. 4, August 1969, pp. 30-35.
17. ACI Committee 343, *Analysis and Design of Reinforced Concrete Bridge Structures*, Report 343-77, American Concrete Institute, Detroit, Michigan, 1977, pp. 73-80.
18. PCI Committee on Prestress Losses, "Recommendations for Estimating Prestress Losses," PCI JOURNAL, V. 20, No. 4, July-August 1975, pp. 43-75.
19. Trost, H., "Auswirkungen des Superpositionsprinzips auf Kriech- und Relaxationsprobleme bei Beton und Spannbeton," *Beton- und Stahlbetonbau*, V. 62, No. 10, 1967, pp. 230-238 and No. 11, 1967, pp. 261-269.
20. Bažant, Z. P., "Prediction of Concrete Creep Effects Using Age-Adjusted Effective Modulus Method," *ACI Journal*, V. 69, No. 4, April 1972, pp. 212-217.
21. ACI Committee 209, "Prediction of

Creep, Shrinkage and Temperature Effects in Concrete Structures," ACI Special Publication SP-76, American Concrete Institute, Detroit, Michigan, 1982, pp. 193-300.
22. Comité Euro-International du Béton (CEB) — Fédération Internationale de la Précontrainte (FIP), *Model Code for Concrete Structures*, CEB, Paris, France, 1978, 348 pp.
23. Favre, R., Beeby, A. W., Falkner, H., Kopma, M., and Schiessel, P., *CEB Design Manual on Cracking and Deformations*, École Polytechnique Fédérale de Lausanne, Switzerland, 1985.
24. Magura, D. D., Sozen, M. A., and Siess, C. P., "A Study of Stress Relaxation in Prestressing Reinforcement," PCI JOURNAL, V. 9, No. 2, April 1964, pp. 13-57.
25. Ghali, A., and Treviño, J., "Relaxation of Steel in Prestressed Concrete," PCI JOURNAL, V. 30, No. 5, September-October 1985, pp. 82-94.
26. Elbadry, M. M., and Ghali, A., *User's Manual and Computer Program CPF: Cracked Plane Frames in Prestressed Concrete*, Research Report No. CE85-2, Department of Civil Engineering, The University of Calgary, Calgary, Alberta, Canada, January 1985. Program is available on diskettes for IBM microcomputers.
27. Elbadry, M. M., "Serviceability of Reinforced Concrete Structures," PhD Thesis, Department of Civil Engineerng, The University of Calgary, Calgary, Alberta, Canada, November 1988, 294 pp.
28. Aparicio, A. C., Arenas, J. J., and Alonso, C., "Examples of Moment Redistribution in Continuous Partially Prestressed Bridges," *International Symposium on Nonlinearity and Continuity in Prestressed Concrete*, Proceedings V. 2, University of Waterloo, Waterloo, Canada, July 4-6, 1983, pp. 185-204.
29. Carnahan, B., Luther, H. A., and Wilkes, J. O., *Applied Numerical Methods*, John Wiley and Sons, Inc., New York, N.Y., 1969, 604 pp.

* * *

METRIC (SI) CONVERSION FACTORS

1 in. = 25.4 mm	1 kip = 4.448 kN
1 in.^{2} = 645.2 mm^2	1 psi = 6.895 × 10^{-3} MPa
1 in.^{3} = 0.0000164 m^3	1 ksi = 6.895 MPa
1 in.^{4} = 416231 mm^4	1 kip-ft = 1.356 kN-m
1 ft = 0.3048 m	1 kip/ft = 14.594 kN/m

NOTE: Discussion of this article is invited. Please submit your comments to PCI Headquarters by October 1, 1989.

APPENDIX A — STRESS AND STRAIN IN A CROSS SECTION

Consider a cross section made of a homogeneous elastic material subjected to a normal force N at an arbitrary reference point O and a bending moment M. Assuming that plane cross sections remain plane, the strain and stress at any fiber at a distance y below O can be expressed as:

$$\epsilon = \epsilon_0 + \psi y; \quad \sigma = E(\epsilon_0 + \psi y) \tag{A1 and 2}$$

where E is the modulus of elasticity, ϵ_0 is the strain at O and ψ $(= d\epsilon/dy)$ is the curvature (the slope of the strain diagram); see Fig. 6b. Equilibrium requires:

$$N = \int \sigma dA; \quad M = \int \sigma y \, dA \tag{A3 and 4}$$

Substitution of Eq. (A2) into (A3) and (A4) gives:

$$N = A\,\sigma_0 + B\,\gamma; \quad M = B\,\sigma_0 + I\,\gamma \tag{A5}$$

where A, B and I are the area of the cross section, and its first and second moments about an axis through O; σ_0 $(= E\,\epsilon_0)$ is the stress at O and γ $(= d\sigma/dy = E\,\psi)$ is the slope of the stress diagram. Eq. (A5) can be used to determine the stress resultants when the stress (or strain) distribution is known. For given N and M, the strain at O and the curvature can be determined by:

$$\epsilon_0 = \frac{IN - BM}{E(AI - B^2)}; \quad \psi = \frac{-BN + AM}{E(AI - B^2)} \tag{A6}$$

When the equations of this appendix are applied to a composite reinforced concrete section with or without prestressing, the symbols A, B and I represent the properties of a transformed section composed of the area of concrete in each part plus the area of reinforcements, each multiplied by its modulus of elasticity and divided by an arbitrary reference modulus, E_{ref}. The reference elasticity modulus can be conveniently taken as the modulus of one of the concrete parts.

* * *

APPENDIX B — DEPTH OF COMPRESSION ZONE IN A FULLY-CRACKED SECTION

Figs. B1a-c show the strain and stress distributions in a composite section due to forces $\{\Delta N, \Delta M\}_{fully\ cracked}$ producing cracking. Prior to applying these forces, the concrete stresses are assumed to be zero in the lower part of the section. The resultant of $\{\Delta N, \Delta M\}_{fully\ cracked}$ is located at an eccentricity e from a reference point O (e is positive when the resultant is situated below O):

$$e = \left(\frac{\Delta M}{\Delta N}\right)_{fully\ cracked} \tag{B1}$$

The strain in any fiber can be expressed by Eq. (A1), but because concrete in tension is ignored, the stresses in concrete and steel are expressed by (go to top of right column):

$$\left.\begin{aligned} \Delta\sigma_c &= E_c\left(1 - \frac{y}{y_n}\right)\Delta\epsilon_0 \quad \text{when } y < y_n \\ \Delta\sigma_c &= 0 \qquad\qquad\qquad\quad \text{when } y \geq y_n \end{aligned}\right\} \tag{B2}$$

$$\Delta\sigma_s = E_s\left(1 - \frac{y_s}{y_n}\right)\Delta\epsilon_0 \tag{B3}$$

where $y_n (= c - d_0)$ is the y coordinate of the neutral axis, with d_0 being the distance from the top fiber to O (positive when O is below top fiber).

The depth c of the compression zone can be determined by taking moments about an axis through the point of application of the resultant of $\{\Delta N, \Delta M\}_{fully\ cracked}$ and equating to zero. This leads to the following equation:

$$e\sum_{i=1}^{m}\left\{A_g\alpha_c(d_c - c) + \sum_{j=1}^{n}[A_s(\alpha_s - \alpha_c)(d_s - c)]_j\right\}_i = \sum_{i=1}^{m}\left\{A_g\alpha_c\left[(d_0 c - d_1^2) + d_c(2d_1 - d_0 - c) + \frac{h^2}{6}\left(\frac{b_1 + 3b_2}{b_1 + b_2}\right)\right] + \sum_{j=1}^{n}[A_s(\alpha_s - \alpha_c)(d_s - c)(d_s - d_0)]_j\right\}_i \tag{B4}$$

For the special case when $\Delta N_{fully\ cracked} = 0$, substitution of Eqs. (B2) and (B3) into (A3) gives:

$$\sum_{i=1}^{m}\left\{A_g\alpha_c(d_c - c) + \sum_{j=1}^{n}[A_s(\alpha_s - \alpha_c)(d_s - c)]_j\right\}_i = 0 \tag{B5}$$

In the above two equations, subscripts c and s refer to concrete and steel, respectively. An additional subscript p or n can be used with s to indicate prestressed or nonprestressed steel. The subscripts i and j refer to a concrete trapezium (Fig. B1d) and a steel layer; m is the total number of trapeziums and n is the number of steel layers included in the ith trapezium; $A_{ci} = E_{ci}/E_{ref}$ and $\alpha_{si} = E_{si}/E_{ref}$. Note that $E_c = 0$ for concrete in the tension zone. Symbols A_{gi} and d_{ci} are the gross area of concrete trapezium i and the distance from its centroid to the extreme compression fiber; for a trapezium of widths b_1 and b_2 and height h (Fig. B1d):

$$A_{gi} = \left[\frac{h}{2}(b_1 + b_2)\right]_i \tag{B6}$$

$$d_{ci} = \left[d_1 + \frac{h}{3}\left(\frac{b_1 + 2b_2}{b_1 + b_2}\right)\right]_i \tag{B7}$$

Solution of Eq. (B4) or (B5) to determine the value of c is best obtained by trial using Newton's iterative technique.[29]

Once c is known, the properties of the cross section A, B and I can be determined leaving out the concrete below the neutral axis and Eqs. (A1), (A2) and (A6) can be used to find the stress and strain changes in a fully cracked section.

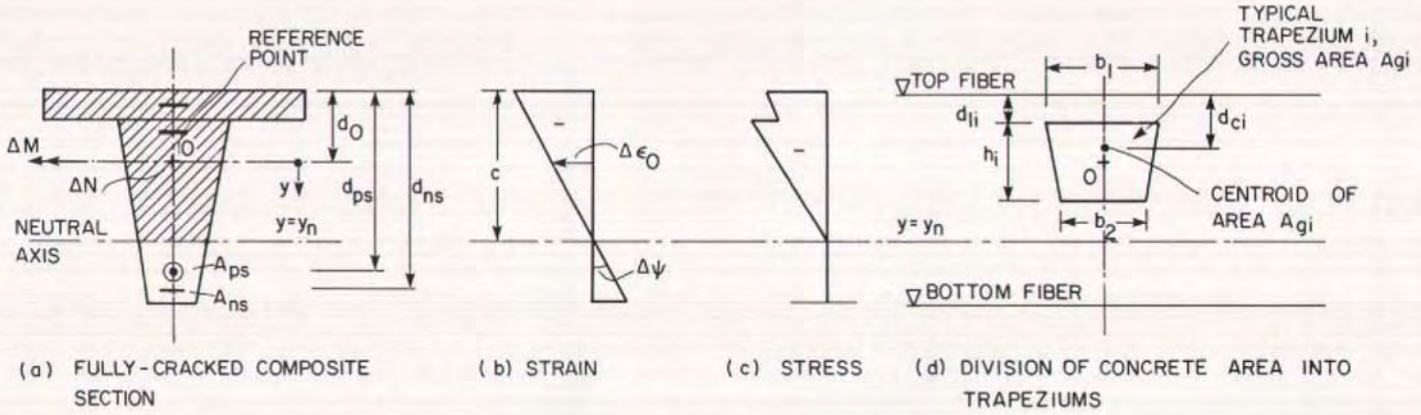

Fig. B1. Concrete strain and stress in a fully cracked section due to $\{\Delta N, \Delta M\}_{\text{fully cracked}}$

APPENDIX C — NOTATION

A and $\bar{A}$ = area of transformed and of age-adjusted transformed sections

B and $\bar{B}$ = first moment of area of transformed and of age-adjusted transformed sections

c = depth of compression zone in a fully cracked section

$\{D\}$ and $\{D^*\}$ = displacement vectors

E and $\bar{E}$ = modulus of elasticity and age-adjusted elasticity modulus

$\{F\}$ and $\{F^*\}$ = vectors of fixed-end forces

$[f]$ and $[\bar{f}]$ = flexibility and age-adjusted flexibility matrices

f_{ct} = tensile strength of concrete

$[H]$ = transformation matrix

I and $\bar{I}$ = moment of inertia of transformed and of age-adjusted transformed sections

k = wobble friction coefficient

M = bending moment

N = normal force

P = absolute value of prestressing force

$[S]$ = stiffness matrix

s_{ij} = length of prestressing tendon between sections i and j

s = average crack spacing

t = time

w = mean crack width

y = coordinate of any section fiber, measured downwards from a reference point O

α = modular ratio

β_1 and β_2 = coefficients, 0.5 or 1 as specified below Eq. (18)

γ = slope of stress diagram

δ = anchor set

Δ = increment or decrement

ϵ = normal strain

ζ = interpolation coefficient

θ_{ij} = change in slope of a prestressing tendon, in radians, between sections i and j

λ = ratio of the initial tensile stress in a tendon to its tensile strength

μ = curvature friction coefficient

σ = stress

$\Delta\sigma_{pr}$ and $\Delta\bar{\sigma}_{pr}$ = intrinsic and reduced relaxation of prestressed steel

ϕ = creep coefficient

χ = aging coefficient

χ_r = relaxation reduction factor

ψ = curvature (slope of strain diagram)

Subscripts

c, ps, ns = concrete, prestressed and nonprestressed steel

cs = shrinkage of concrete

O = reference point

o = initial time

s = steel

* * *